HERON contains contributions based mainly on research work performed in I.B.B.C. and STEVIN and related to strength of materials and structures and materials science.

Jointly edited by:

STEVIN-LABORATORY
of the Department of
Civil Engineering of the
Delft University of Technology,
Delft, The Netherlands
and
I.B.B.C. INSTITUTE TNO
for Building Materials
and Building Structures,
Rijswijk (ZH), The Netherlands.

Secretary:

G. J. van Alphen
Stevinweg 1
P.O. Box 5048
2600 GA Delft, The Netherlands

HERON vol. 25
1980
no. 3

Contents

* Present address: Swiss Federal Institute of Technology, Laboratory for Building Materials, Lausanne, Switzerland.

STOCHASTIC APPROACH TO STUDY THE INFLUENCE OF RATE OF LOADING ON STRENGTH OF CONCRETE

Summary

Although any reliability analysis depends on the entering load and resistance distribution functions, the actual materials behaviour has been neglected in many reliability assessments. Strength of concrete is widely scattered because of the heterogeneity of this composite material. So far no generally accepted theory to describe the stochastic nature of concrete properties is available. Besides of this, hardly anything is known on the influence of rate of loading on the variability, of strength of concrete.

In this paper, a stochastic theory for fracture of concrete materials is presented. This theory is based on physically relevant probability models. It is possible to describe the fracture process not only under monotonically increasing load, buth also under time-dependent loading conditions such as sustained load and repeated load. Moreover, this theory provides a realistic basis for a mathematical formulation of the variability of porous materials. Theoretical predictions are compared with earlier published data. Experiments have been carried out to verify the theoretical approach described in this report. Special emphasis is placed on the influence of rate of loading on the mean strength and the corresponding variability. The rate of loading has been changed by three orders of magnitude and for most series six different rates have been chosen within this range. Specimens of high strength mortar, low strength mortar, lightweight and normal concrete have been tested under compressive and bending load. The distribution function has been evaluated from about 30 individual tests for each chosen condition of loading some experiments to investigate the influence of temperature have been carried out.

The experimental results essentially verify the theoretical approach. The following conclusions were obtained:

- The influence of rate of loading can be described by a power function:

  $$(\bar{\sigma}/\bar{\sigma}_0) = (\dot{\sigma}/\dot{\sigma}_0)^{1/(\beta+1)}$$

  where $\bar{\sigma}_0$ and $\dot{\sigma}_0$ are reference mean value of strength and reference rate of loading respectively, and β is a materials parameter.
- The coefficient of variation does not depend on rate of loading.
- Materials with a low average strength experience a more pronounced strength increase as the rate of loading increases.
- The distribution of strength as determined by three point bending test and under compressive load can be described satisfactorily by Weibull's distribution function.

Stochastic approach to study the influence of rate of loading on strength of concrete

1 Introduction

There are many reports or studies of the fracture behaviour of concrete. Most of them, however, are mainly based on phenomenological observation and various empirical formulae applicable to some limited conditions have been proposed. On the other hand, there are quite few theoretical approaches which can predict satisfactorily the fracture of concrete.

Fundamental theories such as the original one by Griffith [1920] and most of the modification which followed treat only crack initiation at regular flaws in an isotropic and homogeneous solid. But concrete is a very heterogeneous material and fracture initiation is a highly localized phenomenon. Therefore the wide scatter of the test results concerning fracture behaviour of concrete should be considered as a characteristic property which cannot be separated from the physical aspects of this type of materials. As a consequence the nature of the observed phenomena need to be analysed by statistical methods.

At present there are many papers to discuss which kind of statistical distribution function is best suited to describe the distribution function of concrete strength [see for example: D. P. Maynard and S. G. Davis, 1974; R. J. Torrent, 1979]. But it is very difficult to discriminate by a limited number of test results whether the choice of a normal distribution, a log-normal distribution or a typical extreme value distribution is more realistic. Because of the fact that fitting of different distribution functions to existing test results does not provide a clear answer to this problem there is a need to derive appropriate distribution functions on the basis of realistic physical concepts.

Weibull [1939] proposed a statistical theory. He was the first to apply the weakest link concept to fracture phenomena of solids, and he arrived at a distribution function of the smallest values (so-called Weibull's distribution function).

Weibull's approach was especially successful to describe the size effect of brittle fracture of solids. Freudenthal [1968] conjuncted this asymptotic distribution function based on the weakest link model, with the Griffith crack instability criterion to discuss more generally the scatter of fracture phenomena of brittle materials.

Fracture behaviour of concrete materials, however, is quite different from that of idealy or nearly brittle materials. There is a stage of stable crack propagation even under a tensile load [Kaplan, 1961]. Moreover, compressive fracture is caused by accumulation of micro cracks which increase with the compressive load. Therefore another theory which takes into consideration structural aspects of concrete is required in place of purely statistical theories such as the one by Weibull [1939].

Most conventional concrete structures are designed in such a way that concrete has to carry static compressive load. But there is an increasing number of concrete structures or structural elements where the design load is dependent on the behaviour of concrete

under high rate of loading. Typical examples are columns of highway structures, slender off-shore structures, concrete ships and concrete piles used for foundations. The secondary safety containment of nuclear power plants which is designed to resist among other loading conditions missile impact external explosions and seismic loads, is just another example which underlines the necessity to know more about materials properties under high rate of loading.

For a realistic reliability assessment, not only the mean value of strength as function of rate of loading is needed but the distribution function must be known too. So far, limited information on the influence of rate of loading on the average strength can be obtained from the literature. But very little is known on the distribution of strength at high rates of loading. Therefore we shall concentrate in this contribution on the influence of rate of loading on the variability of concrete strength.

Mechanical properties of all materials are dependent on rate of loading. It is well known that strength of steel or plastics increases at higher rates of loading [Mainstone, 1975]. Similar behaviour is observed on brittle materials such as glas [Chandon et al., 1978].

Watstein [1953] has shown among others that compressive strength as well as elastic modulus of concrete increase at high rate of loading. There is a wide scatter of the experimental findings of various authors. But a remarkable increase of compressive strength with increasing rate of loading undoubtedly may be assumed. Similar results have been obtained by measurements of direct tensile strength [Reinhardt 1979] and of bending strength [Zech and Wittmann 1980]. Gupta and Seaman [1975] observed an increase of strength by a factor of 10 under missile impact loading.

A new concept to describe the stochastic nature of failure of concrete has recently been published by Mihashi and Izumi [1977]. On the basis of this approach the influence of temperature, of size of the specimen, and of rate of loading on strength can be explained uniformely.

In the following section on the same basis a stochastic theory to describe fracture of concrete will be outlined. The essential theoretical predictions shall be compared with experimental findings on this report.

2 Stochastic theory for fracture of concrete

2.1 *Assumptions and model*

Roughly speaking, most of the previous studies concerning the fracture behaviour of concrete can be subdivided into the following three groups from the view point of the level.

1. Macroscopic level:
   Characteristic length in the order of 100 mm or more. Typical materials properties to be studied: average stress and strain, strength, nonlinearity of mechanical properties.
2. Submacroscopic level:
   Characteristic length in the order of 1 mm or 10 mm. Typical materials properties to be studied: local stress and strain, crack formation, failure process, fracture mechanism.

3. Microscopic level:
   Characteristic length in the order of 10^{-1} mm or less. Typical materials properties to be studied: microstress and microstrain, hydration, porosity, structure.

The characteristic macroscopic phenomena are caused by submacroscopic failure and remarkably affected by the factors on the microscopic level. Concrete materials i.e. cement paste, mortar and concrete contain enough submacroscopic material defects such as voids (entrapped air), flaws, shrinkage cracks and interfacial cracks. Therefore the stress distribution in the solids is remarkably disturbed by these defects. And it is well known that the failure process is highly affected by some bigger material defects among them. Under uniaxial load the failure behaviour around each defect is rather independent of the rest of the materials structure with the exception of direct neighbouring pores. The failure process can be assumed to be the same of many microprocesses. Until fracture occurs a series of typical states of crack propagation is followed.

The failure process highly depends on the material and the loading condition. Cement paste under tensile load behaves just like porous rock. Fracture occurs in a quite brittle manner and there are not stable states with crack initiation. The specimen fractures immediately when a crack initiates from a pre-existing micro crack.

Concrete and mortar under compressive load, however, are not fractured in such a way. There are some stable states with submacroscopic cracks and the failure is caused by the accumulation of many cracks.

From the view point of the microscopic level, the fracture of concrete materials may be caused by a series of local failure processes in the phase of hydratation products of cement and interfaces. When a failure criterion is satisfied in one part of the phase, a crack is created. Its extension and the connection with other cracks cause eventually fracture. This holds true even under tensile load [Higgins and Baily, 1976].

On the basis of these facts, the following assumptions may be introduced for the mathematical treatment.

a. The concrete system may be considered to consist of a group of m elements with two or three phases which are linked in series. (In the case of fracture under multi-axial compressive load, the structural element must be reconsidered according to the failure process). This situation is shown schematically in Fig. 2.1.
b. Each phase consists of n units which contain a circular crack. This model may be representative for hardened cement paste and is shown in Fig. 2.2.
c. The dimensions of a circular crack may be evaluated by the equivalent crack length $2c^2$: where c is a fracture factor.

   $c = g(s, l, t)$

   c depends on s, which is a micro-stress disturbance coefficient caused by material defects, on $2l$ the microcrack length (which may be related to micropore size) and on time t, s and l are random variables and mutually independent. When the relative fracture factor of a microcrack under a given stress is estimated, the following equation is obtained on the basis of elementary fracture mechanics:

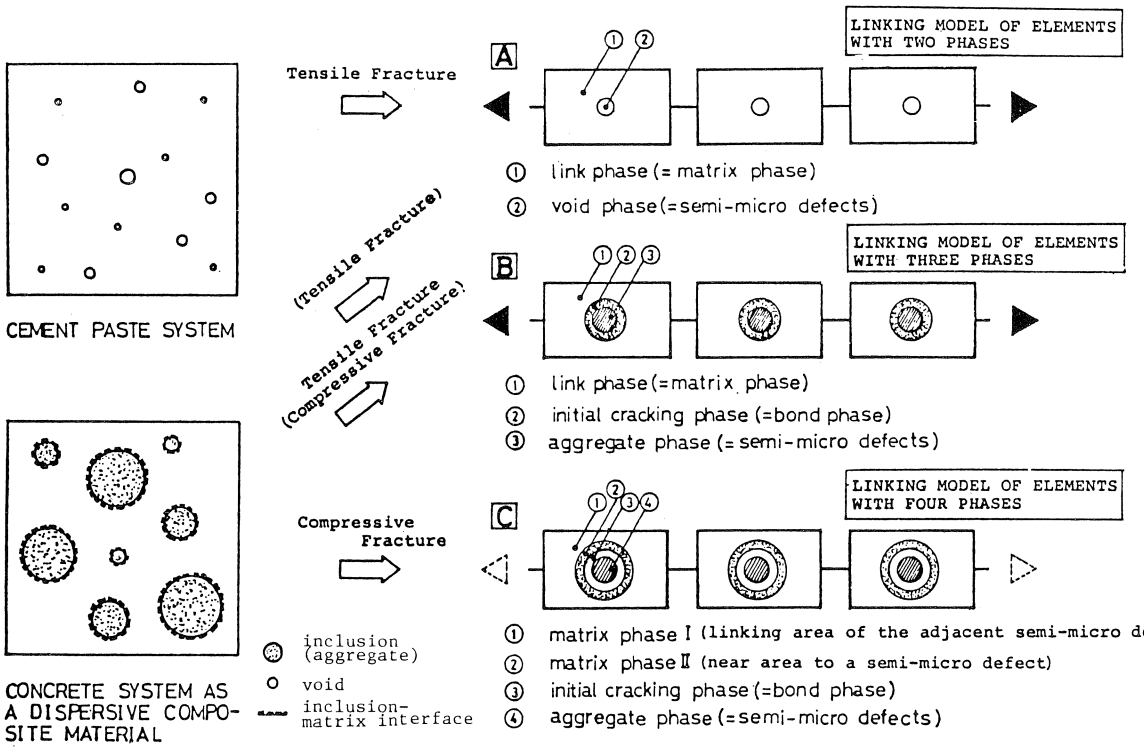

Fig. 2.1. Linking model of elements (in series).

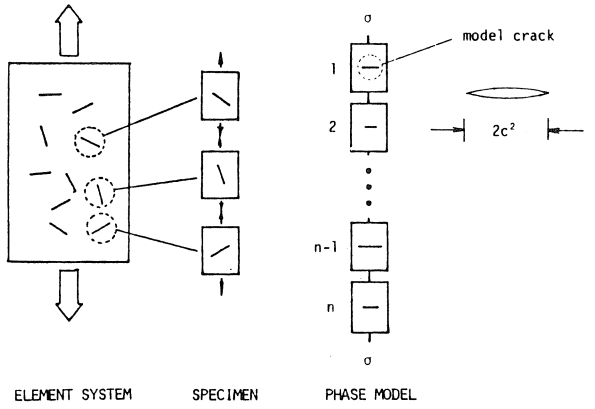

Fig. 2.2. Hardened cement paste phase model.

$$c = ks\sqrt{\frac{l}{Ey}} \tag{2.1}$$

Where E is Young's Modulus, y is the surface energy and k is a constant. If only a specific crack length such as the expected maximum micro crack length ($2\bar{l}$) is considered, the density function of the fracture factor is described as follows.

$$f_c(c) = \frac{1}{k}\sqrt{\frac{Ey}{\bar{l}}} \cdot f_s(s) \tag{2.2}$$

d. Different failure processes are described in Fig. 2.3. For each state, only the micro stress distribution is changed by submicroscopic cracking. In type A, there are no stable states for crack formation. In type B, the internal micro stress distribution of state 1 is different from the initial state. Fracture of the specimen is dominated not only by the initial state but also by the state 1. In type C finally the failure process is treated much more comprehensive.

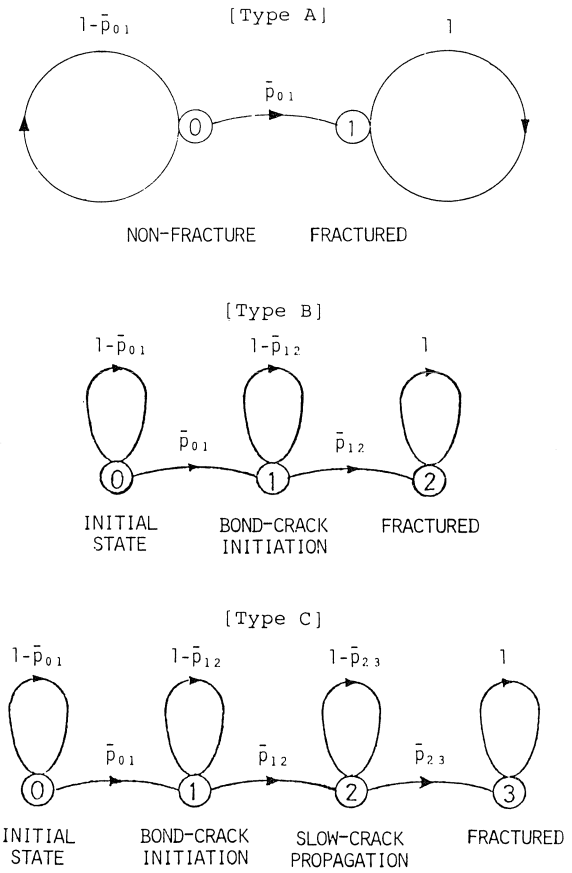

Fig. 2.3. Mathematical models - Transition line graph.

e. The distribution of material defects and the characteristic properties of each element are statistically equal over the whole region.

2.2 *Strength under monotonically increasing load*

2.2.1 Failure of material of type A

According to the theory of rate process, the rate of crack initiation on an atomic scale is given by the following equation:

$$r=\frac{kT}{h}\exp\left[-\{U_0-\varphi(\sigma_l)\}/kT\right] \tag{2.3}$$

It is assumed that $\varphi(\sigma_l) \gg kT$, where φ is an increasing function of σ_l and σ_l is the local stress at the area of interest. U_0 = activation energy in the non-stressed material, k = Boltzmann constant, h = Planck constant and T = absolute temperature. The activation energy $U(\sigma) = U_0 - \varphi(\sigma_l)$ is dependent on the type of the objective phenomena. In the case of brittle fracture under a static load, the function $U(\sigma)$ is given by eq. (2.4) according to the theory of heterogeneous nucleation [Yokobori, 1974].

$$U(\sigma)=U_b-\frac{1}{n_b}\ln(q\sigma) \tag{2.4}$$

Where U_b and n_b are material constants, q is the local stress concentration coefficient that means $q\sigma$ is the local stress:

$$q\sigma=\alpha_b\sqrt{\pi l\sigma}=\alpha_b K$$

where α_b is constant, and K = stress intensity factor. The same function is given in creep fracture, too. Hence the eq. (2.3) can be rewritten:

$$r=\frac{kT}{h}\exp\left(-U_b/kT\right)(q\sigma)^{\frac{1}{n_b kT}} \tag{2.5}$$

Since a crack is most likely to nucleate at the zone of stress concentration, the rate of real crack nucleation I may be assumed to be proportional to the number of molecules in the vicinity of the tip of the pre-existing crack. That means the rate is proportional to the crack length.

Therefore the following equation is obtained:

$$I=VZr \tag{2.6}$$

where Z is the number of molecules in the stress concentrated zone and V is the effective volume and not the total volume of the specimen.

Let $\mu_i(t)\cdot dt$ be the probability of fracture initiation from a unit i between a given time t and $t+dt$. The mean value $\bar{\mu}_i(t)$ for a large number of n is then given by:

$$\begin{aligned}\bar{\mu}_i(t) &= \int_0^\infty \mu_i(t)\cdot g(\mu_i)\,d\mu_i \\ &= \int_0^\infty \mu_i(t)\cdot f_c(c)\cdot dc\end{aligned} \tag{2.7}$$

From eq. (2.6), $\mu_i(t)$ is described by eq. (2.8) because of $\mu_i(t) \propto I$.

$$\mu_i(t) = Z'A(T)(c\cdot\sigma)^{\beta}\cdot l \tag{2.8}$$

where $A(T)$ and β are material constants dependent on the absolute temperature and Z' is a material constant. From eqs. (2.7) and (2.8) it follows:

$$\bar{\mu}_i(t) = \int_0^{\infty} Z'A(T)(c\cdot\sigma)^{\beta} l\cdot f_c(c)\cdot \mathrm{d}c \tag{2.9}$$

In the simple case when only one specific crack length $(2\bar{l})$ is considered, the following equation is obtained.

$$\bar{\mu}_i(t) = \bar{Z}A(Ey)^{-\beta/2}\cdot \bar{l}^{\beta/2+1}\sigma(t)^{\beta}\int_0^{\infty} s^{\beta} f_s(s)\cdot \mathrm{d}s \tag{2.10}$$

because

$$f_c(c)\cdot \mathrm{d}c \propto f_s(s)\cdot \mathrm{d}s$$

If $\bar{p}\cdot \mathrm{d}t$ is the mean value of the probability of fracture occurrence in one element within a given time interval t and $t+\mathrm{d}t$, the probability $\hat{P}(t)$ that no fracture occurs before t in any units is obtained by eq. (2.11).

$$\hat{P}(t) = \exp\left(-\int_0^{t} \bar{p}(t)\cdot \mathrm{d}t\right) \tag{2.11}$$

where $\bar{p}(t) = n\bar{\mu}_i(t)$.

Hence

$$\begin{aligned}\bar{p}(t) &= n\bar{Z}A(Ey)^{-\beta/2}\cdot \bar{l}^{\beta/2+1}\sigma(t)^{\beta}\int_0^{\infty} s^{\beta} f_s(s)\cdot \mathrm{d}s \\ &= L\sigma(t)^{\beta}\end{aligned} \tag{2.12}$$

where

$$L = n\bar{Z}A(Ey)^{-\beta/2}\cdot \bar{l}^{\beta/2+1}R$$

and

$$R = \int_0^{\infty} s^{\beta} f_s(s)\cdot \mathrm{d}s$$

Therefore the non-fracture probability under uniformly increasing tensile stress is given by eq. (2.13).

$$P(\sigma) = \exp\left\{-\frac{mL}{(\beta+1)\dot{\sigma}}\sigma^{\beta+1}\right\} \tag{2.13}$$

where m is the specimen size parameter and $\dot{\sigma}$ is the stress rate. And the probability density function of strength $q(\sigma)$ is obtained as follows.

$$q(\sigma) = \frac{mL}{\dot{\sigma}} \sigma^{\beta} \exp\left\{-\frac{mL}{(\beta+1)\dot{\sigma}} \sigma^{\beta+1}\right\} \tag{2.14}$$

Hence the mean value of strength $\bar{\sigma}$ is given by eq. (2.15).

$$\bar{\sigma} = \left\{\frac{(\beta+1)\dot{\sigma}}{mL}\right\}^{1/(\beta+1)} \cdot \Gamma\left(\frac{\beta+2}{\beta+1}\right) \tag{2.15}$$

where Γ is the Gamma function. And the peak value of the function $q(\sigma)$ is expressed as follows.

$$\bar{\sigma}_m = \left(\frac{\beta\dot{\sigma}}{mL}\right)^{\frac{1}{\beta+1}} \tag{2.16}$$

Eq. (2.15) or (2.16) indicate that large values of L and m decrease the value of $\bar{\sigma}$. It should be noted, moreover, these equations lead to explanations of kinetic effects of stress rate and temperature which could not be explained by usual extreme probability theory. The variance (or dispersion) of strength is obtained by eq. (2.17):

$$V^2(\sigma) = \left\{\frac{(\beta+1)\dot{\sigma}}{mL}\right\}^{2/(\beta+1)} \left\{\Gamma\left(\frac{\beta+3}{\beta+1}\right) - \Gamma^2\left(\frac{\beta+2}{\beta+1}\right)\right\} \tag{2.17}$$

This predicts that large values of L and m decrease the scattering of strength.

From eqs. (2.15) and (2.17) the following equation can be deduced:

$$\frac{V(\sigma)}{\bar{\sigma}} = \frac{\left\{\Gamma\left(\frac{\beta+3}{\beta+1}\right) - \Gamma^2\left(\frac{\beta+2}{\beta+1}\right)\right\}^{1/2}}{\Gamma\left(\frac{\beta+2}{\beta+1}\right)} \tag{2.18}$$

Eq. (2.18) means that the coefficient of variation is not influenced by the rate of loading, but it is rather a constant for a given material. In the same way, the mean value of flexural strength under third point loading is obtained as follows:

$$\bar{\sigma} = \left\{\frac{3(\beta+1)^3\dot{\sigma}_0}{m \cdot abh \cdot (\beta+3)L}\right\}^{\frac{1}{\beta+1}} \Gamma\left(\frac{\beta+2}{\beta+1}\right) \tag{2.19}$$

where a is the half length of the span simply supported, while b is the width and h is the height of the beam, and $\dot{\sigma}_0$ is the stress rate at the outer fiber in the center of the span.

2.2.2 Failure of a material of type B and type C

Generally speaking, it is more suitable to describe concrete fracture phenomena as successive events. In such a case, let $P_i(t)$ be the probability that the state of an element has transformed into the stage i of the successive stochastic processes at a given time t. Then the following differential equations are obtained.

$$\mathrm{d}P_0(t)/\mathrm{d}t = -\bar{p}_{01}(t)P_0(t) \tag{2.20}$$

$$\mathrm{d}P_i(t)/\mathrm{d}t = -\bar{p}_{i,i+1}(t)P_i(t) + \bar{p}_{i-1,i}(t)P_{i-1}(t) \tag{2.21}$$

where

$$\bar{p}_{ij}(t) = L_i \cdot |\sigma|^{\beta}$$

and

$$L_i = n\bar{Z}(E\dot{\varepsilon})^{-\beta/2} \cdot \bar{I}^{\beta/2+1} AR_i$$

indicating the probability that an element makes a transition from stage i to stage j in a unit interval at a certain time t. From eq. (2.21) under the initial condition:

$$P_0(0) = 1,\ P_i(0) = 0 (i \neq 0)$$

one can obtain the following equation:

$$P_i(t) = \exp\left\{-\int_0^t \bar{p}_{i,i+1}(t) \cdot \mathrm{d}t\right\} u_i(t) \tag{2.22}$$

where

$$u_i(t) = \int_0^t \left\{\bar{p}_{li}(t) \exp\left[\int_0^t \{\bar{p}_{i,i+1}(t) - \bar{p}_{li}(t)\} \cdot \mathrm{d}t\right] \cdot u_l(t)\ \mathrm{d}t\right\} \tag{2.23}$$

and

$$l = i - 1$$

and the initial conditions concerning $u_i(t)$ are

$$u_i(0) = 0;\ i \geq 1$$

Under uniformly increasing stress, eq. (2.22) is rewritten as follows:

$$P_i(t) = \exp\left\{\frac{-L_i \cdot \sigma^{\beta+1}}{(\beta+1)\dot{\sigma}}\right\} \int_0^{\sigma} \left[\frac{L_l \cdot \sigma^{\beta}}{\dot{\sigma}} \exp\left\{\frac{L_i - L_l}{(\beta+1)\dot{\sigma}} \sigma^{\beta+1}\right\} u_l(\sigma)\right] \mathrm{d}\sigma \tag{2.24}$$

Now the probability that no fracture occurs below a given stress within a given element is written for the two types of model material as follows:

$$\overset{e}{P}(\sigma) = \sum_{i=0}^{j-1} P_i(\sigma) \tag{2.25}$$

where $j = 2$ for type B and $j = 3$ for type C and the non-fracture probability of the specimen can be expressed as $P(s) = \{\overset{e}{P}(\sigma)\}^m$.

Therefore the following equation is obtained.

$$P(\sigma) = \left[\sum_{i=0}^{j-1} \prod_{k=0}^{j-1} \frac{L_k}{(L_i - L_k)} \exp\left\{\frac{-L_i}{(\beta+1)\dot{\sigma}} \sigma^{\beta+1}\right\}\right]^m \tag{2.26}$$

where according to the type of model material $j = 2$ or 3 and $k \neq i$.

Then the mean values of fracture strength in the case of type B is obtained as follows:

$$\bar{\sigma} = \left\{\frac{(\beta+1)\dot{\sigma}}{mL_0}\right\}^{\frac{1}{\beta+1}} \left[\frac{L_1}{mL_0} \cdot \Gamma\left(\frac{2\beta+3}{\beta+1}\right) + \frac{\{(2m-1)\cdot L_0 - L_1\}\cdot L_1}{2m^2L_0^2} \cdot \right.$$
$$\left. \cdot \Gamma\left(\frac{3\beta+4}{\beta+1}\right) + \frac{m^2L_0^2 + (1-3m)\cdot L_0L_1 + L_1^2}{6m^2L_0^2} \cdot \Gamma\left(\frac{4\beta+5}{\beta+1}\right)\right] \tag{2.27}$$
$$= \left\{\frac{(\beta+1)\dot{\sigma}}{mL_0}\right\}^{\frac{1}{\beta+1}} \cdot F(\lambda_1, m, \beta)$$

where

$$\lambda_1 = L_1/L_0$$

and for type C another expression is found in a same way.

2.3 *Strength under sustained load*

2.3.1 Fracture without consideration of aging effect

2.3.1.1 Fracture under sustained tensile or bending load

The probability that no fracture occurs in the purely brittle specimen like type A before time t, is defined by $P(t)$ as follows:

$$P(t) = \exp\left(-\int_0^t mL\sigma^\beta \, dt\right) = \exp\,(-mL\sigma^\beta t) \tag{2.28}$$

Therefore the fracture probability $D(t)$ is

$$D(t) = 1 - \exp\,(-mL\sigma^\beta t) \tag{2.29}$$

The probability density function of fracture strength $q(t)$ is

$$q(t)\cdot dt = mL\sigma^\beta \exp\,(-mL\sigma^\beta t)\cdot dt \tag{2.30}$$

The mean value $\bar{t}$ of fracture time is described by

$$\bar{t} = \int_0^\infty t\cdot q(t)\cdot dt = \int_0^\infty mL\sigma^\beta t \exp\,(-mL\sigma^\beta t)\cdot dt$$
$$= \frac{1}{mL\sigma^\beta}\int_0^\infty X\cdot\exp\,(-X)\cdot dX$$

where

$$X = mL\sigma^\beta t$$

Finally we can get the following equation.

$$\bar{t} = \frac{1}{mL\sigma^\beta}\Gamma(2) \tag{2.31}$$

and we get far the related legitime of a specimen:

$$\bar{t}/\bar{t}_0 = \left(\frac{\sigma_0}{\sigma}\right)^{\beta} \tag{2.32}$$

or what is equivalent with eq. (2.32)

$$\sigma/\sigma_0 = (\bar{t}_0/\bar{t})^{1/\beta} \tag{2.33}$$

Therefore

$$\ln \sigma/\sigma_0 = \frac{-1}{\beta} \ln \bar{t}/\bar{t}_0 \tag{2.34}$$

Then the variance $V^2(t)$ is obtained as follows:

$$V^2(t) = \int_0^{\infty} t^2 \cdot q(t) \cdot \mathrm{d}t - (\bar{t})^2 \tag{2.35}$$

$$= \frac{1}{(mL\sigma^{\beta})^2} \{\Gamma(3) - \Gamma^2(2)\}$$

Hence

$$\frac{V(t)}{\bar{t}} = \frac{\{\Gamma(3) - \Gamma^2(2)\}^{1/2}}{\Gamma(2)} \tag{2.36}$$

2.3.1.2 Fracture under sustained compressive load

Since the failure process of concrete is not purely brittle because of its heterogeneity and the different crack arresting mechanisms, the probability $P_i(t)$ that the state of an element has been transformed into the stage i of the successive stochastic processes at a given time t, has to be considered. One can obtain $P_i(t)$ for a model material of type B or type C in an analogous way as described for a material of type A by eq. (2.28):

$$P_i(t) = \exp\left\{-\int_0^t \bar{p}_{i,i+1}(t)\, \mathrm{d}t\right\} u_i(t) \tag{2.37}$$

where $\bar{p}_{ij}$ means the probability that an element makes a transition from stage i to j in a unit interval at a certain time t.

$$u_i(t) = \int_0^t \left\{\bar{p}_{li}(t) \cdot \exp\left[\int_0^t \left\{\bar{p}_{i,i+1}(t) - \bar{p}_{li}(t)\right\} \mathrm{d}t\right] u_l(t)\right\} \mathrm{d}t \tag{2.38}$$

where

$$u_0(t) = 1;\ l = i - 1$$

Therefore $(i = 1)$:

$$u_1(t) = \int_0^t \left\{\bar{p}_{01}(t) \cdot \exp\left[\int_0^t \left\{\bar{p}_{12}(t) - \bar{p}_{01}(t)\right\} \mathrm{d}t\right]\right\} \mathrm{d}t$$

We assume that the probability $\bar{p}_{ij}(t)$ can be described by eq. (2.12).

$$\bar{p}_{ij}(t) = L_i|\sigma|^{\beta} \tag{2.39}$$

where

$$L_i = n\bar{Z}A(Ey)^{-\beta/2}\,\bar{l}^{\beta/2+1}\cdot R_i$$

Hence it follows for $i=0$ and $i=1$:

$$\bar{p}_{01}(t) = L_0\cdot|\sigma|^{\beta};\qquad \bar{p}_{12}(t) = L_1|\sigma|^{\beta}$$

Therefore $u_1(t)$ can be rewritten:

$$u_1(t) = \int_0^t [L_0|\sigma|^{\beta}\cdot\exp\{(L_1-L_0)\cdot|\sigma|^{\beta}\cdot t\}]\,\mathrm{d}t$$

$$= \frac{L_0}{(L_1-L_0)}[\exp\{(L_1-L_0)|\sigma|^{\beta}t\}-1]$$

Accordingly we obtain the probability that the state of one element has been transformed from eq. (2.37):

$$P_0(t) = \exp(-L_0\cdot|\sigma|^{\beta}\cdot t)$$

$$P_1(t) = \exp\left(-\int_0^t L_1|\sigma|^{\beta}\,\mathrm{d}t\right)\cdot\frac{L_0}{(L_1-L_0)}[\exp\{(L_1-L_0)|\sigma|^{\beta}t\}-1]$$

$$= \frac{L_0}{(L_1-L_0)}[\exp(-L_0|\sigma|^{\beta}\cdot t)-\exp(-L_1|\sigma|^{\beta}\cdot t]$$

The probability $\overset{e}{P}(t)$ that the element is not fractured before a given time t, is then obtained as follows:

$$\overset{e}{P}(t) = P_0(t)+P_1(t)$$

$$= \frac{1}{(L_1-L_0)}\{L_1\exp(-L_0|\sigma|^{\beta}t)-L_0\exp(-L_1|\sigma|^{\beta}\cdot t)\} \tag{2.40}$$

The probability density function of the fracture time of an element is then given by:

$$\overset{e}{q}(t) = \frac{L_0L_1\sigma^{\beta}}{(L_1-L_0)}\{\exp(-L_0|\sigma|^{\beta}\cdot t)-\exp(-L_1|\sigma|^{\beta}\cdot t)\} \tag{2.41}$$

and mean value of the fracture time is

$$\bar{t}_e = \frac{(L_0+L_1)}{L_0L_1|\sigma|^{\beta}}\Gamma(2) = \frac{(L_0/L_1+1)}{L_0|\sigma|^{\beta}}\Gamma(2) \tag{2.42}$$

The non-fracture probability of a specimen with m elements can be expressed by the relation

$$P(t) = \{\overset{e}{P}(t)\}^m$$

Consequently the following equation is obtained:

$$P(t) = \frac{1}{(L_1 - L_0)^m} \{L_1 \exp(-L_0|\sigma|^\beta t) - L_0 \exp(-L_1|\sigma|^\beta t)\}^m \tag{2.43}$$

The probability density function of the fracture time can be written as follows:

$$\begin{aligned} q(t) &= \frac{mL_0L_1|\sigma|^\beta}{(L_1 - L_0)^m} \{L_1 \exp(-L_0|\sigma|^\beta t) - L_0 \exp(-L_1|\sigma|^\beta t)\}^{m-1} \\ &\quad \cdot \{\exp(-L_0|\sigma|^\beta t) - \exp(-L_1|\sigma|^\beta t)\} \\ &= mL_0\sigma^\beta \cdot \exp(-mL_0\sigma^\beta t) \left[L_1\sigma^\beta t + L_1 \cdot \{(2m-1) \cdot L_0 - L_1\}\sigma^{2\beta} \frac{t^2}{2}\right. \\ &\quad \left. + \{L_1^2 + (1-3m) \cdot L_1L_0 + m^2L_0^2\}\sigma^{3\beta} \frac{t^3}{6}\right] \end{aligned} \tag{2.44}$$

The mean value of the fracture time is described by eq. (2.45).

$$\begin{aligned} \bar{t} &= \frac{1}{m^2L_0\sigma^\beta} \left[\frac{L_1}{L_0} \cdot \Gamma(3) + \frac{\{(2m-1) \cdot L_0L_1 - L_1^2\}}{2mL_0^2} \Gamma(4)\right. \\ &\quad \left. + \frac{\{L_1^2 + (1-3m) \cdot L_1L_0 + m^2L_0^2\}}{6mL_0^2} \Gamma(5)\right] \\ &= \frac{1}{m^2L_0\sigma^\beta} \cdot \Gamma(\lambda_1, m) \end{aligned} \tag{2.45}$$

where

$$\lambda_1 = L_1/L_0$$

2.3.2 Consideration of the aging effect on the fracture behaviour of concrete from the view point of a stochastic theory

Young's modulus E, surface energy γ, and pre-existing crack length $\bar{l}$ may be functions of the age of specimens. The time-dependence may be described by the following equations:

$$E(\tau) = E_1\tau^{a1} \tag{2.46}$$

$$\gamma(\tau) = \gamma_1\tau^{a2} \tag{2.47}$$

$$\bar{l}(\tau) = \bar{l}_1/\tau^{a3} \tag{2.48}$$

where $a1$, $a2$ and $a3$ are materials parameters which are affected by water-cement ratio and type of cement etc. From eq. (2.12), the term L can be subdivided into two components, i.e.

$$L = \bar{L} \cdot L(t)$$

Then $L(t)$ is given by:

$$L(t) = (Ey)^{-\beta/2}\,\bar{I}^{(\beta+2)/2} = C_1 \tau^{-a} \tag{2.49}$$

where

$$C_1 = (E_1 y_1)^{-\beta/2}\,\bar{I}_1^{(\beta+2)/2} \quad \text{and} \quad a = \tfrac{1}{2}\{\beta(a1 + a2) + (\beta+2)\cdot a3\}$$

On the assumption that β is not affected by the age of a specimen and that $\dot{\sigma}$ is high enough in comparison with the change of materials properties as function of age τ, the aging effect on the strength is:

$$\bar{\sigma} = \left\{\frac{(\beta+1)\dot{\sigma}}{m\bar{L}C_1}\right\}^{\frac{1}{\beta+1}} \Gamma\left(\frac{\beta+2}{\beta+1}\right) \tau^{\frac{a}{(\beta+1)}}$$

$$\bar{\sigma}_m = \left\{\frac{\beta\dot{\sigma}}{m\bar{L}C_1}\right\}^{\frac{1}{\beta+1}} \tau^{\frac{a}{\beta+1}} \tag{2.50}$$

If we consider specimens with the same w/c ratio, the strength ratio is

$$\eta = \bar{\sigma}(\tau)/\bar{\sigma}(\tau_0) = (\tau/\tau_0)^{\frac{a}{(\beta+1)}} \tag{2.51}$$

Under a sustained load, the non-fracture probability may be obtained by eq. (2.52).

$$P(t, \tau_0) = \exp\left\{-\int_0^t m\bar{L}\cdot L(t, \tau_0)\sigma^{\beta}\,\mathrm{d}t\right\} \tag{2.52}$$

where

$$L(t, \tau_0) = C_1(t+\tau_0)^{-a}$$

and $\tau_0 =$ the age of the specimen at which the load has been applied. Hence

$$P(t, \tau_0) = \exp\left\{\frac{m\bar{L}C_1\sigma^{\beta}}{(1-a)}\,\tau_0^{1-a}\right\} \exp\left\{\frac{-m\bar{L}C_1\sigma^{\beta}}{(1-a)}\,(t+\tau_0)^{1-a}\right\}; \qquad (a \neq 1) \tag{2.53}$$

The probability density function is as follows.

$$q(t, \tau_0) = m\bar{L}C_1\sigma^{\beta}\cdot\exp\left\{\frac{m\bar{L}C_1\sigma^{\beta}}{(1-a)}\,\tau_0^{1-a}\right\}(t+\tau_0)^{-a}\cdot\exp\left\{-\frac{m\bar{L}C_1\sigma^{\beta}}{(1-a)}\cdot(t+\tau_0)^{1-a}\right\} \tag{2.54}$$

Therefore the mean value of fracture time is described by eq. (2.55):

$$\bar{t}(\tau_0, \sigma) = m\bar{L}C_1\sigma^{\beta}\cdot\exp\left\{\frac{m\bar{L}C_1\sigma^{\beta}}{(1-a)}\,\tau_0^{1-a}\right\}\int_0^{\infty} t(t+\tau_0)^{-a}\cdot\exp\left\{-\frac{m\bar{L}C_1\sigma^{\beta}}{(1-a)}\,(t+\tau_0)^{1-a}\right\}\mathrm{d}t$$

$$= \exp\left\{\frac{m\bar{L}C_1\sigma^{\beta}}{(1-a)}\,\tau_0^{1-a}\right\}\left[\left\{\frac{(1-a)}{m\bar{L}C_1\sigma^{\beta}}\right\}^{\frac{1}{1-a}}\cdot\Gamma\left(\frac{2-a}{1-a}, \frac{m\bar{L}C_1\sigma^{\beta}}{(1-a)}\,\tau_0^{1-a}\right)\right.$$

$$\left. - \tau_0\Gamma\left(1, \frac{m\bar{L}C_1\sigma^{\beta}}{(1-a)}\,\tau_0^{1-a}\right)\right] \tag{2.55}$$

where $\Gamma(b, z)$ is the Incomplete Gamma Function and an asymptotic expansion of this function is as follows (where $b>0$):

$$\Gamma(b,z) = z^{b-1} \exp(-z) \left\{1 + \frac{b-1}{z} + \frac{(b-1)(b-2)}{z^2} + \frac{(b-1)(b-2)(b-3)}{z^3} + \dots\right\} \tag{2.56}$$

If we consider the expansion until the third term, the mean value of fracture time may be described by eq. (2.57).

$$\bar{t} = \frac{\tau_0^a}{m\bar{L}C_1\sigma^\beta}\left(1 + \frac{a}{m\bar{L}C_1\tau_0^{1-a}\sigma^\beta}\right) \tag{2.57}$$

In the case of old specimens, eq. (2.57) may be rewritten as:

$$\bar{t} = \frac{1}{mL\sigma^\beta}\left(1 + \frac{a}{mL\sigma^\beta\tau_0}\right)$$

where

$$L = \bar{L}C_1\tau_0^{-a}$$

If $a=1$, eq. (2.53) should be replaced by eq. (2.58):

$$\begin{aligned} P(t, \tau_0) &= \exp(m\bar{L}C_1\sigma^\beta \ln \tau_0) \exp\{-m\bar{L}C_1\sigma^\beta \ln(t+\tau_0)\} \\ &= \exp(m\bar{L}C_1\sigma^\beta \ln \tau_0)(t+\tau_0)^{-m\bar{L}C_1\sigma^\beta} \end{aligned} \tag{2.58}$$

and the probability density function is then given by:

$$q(t, \tau_0) = m\bar{L}C_1\sigma^\beta \cdot \exp(m\bar{L}C_1\sigma^\beta \cdot \ln \tau_0)(t+\tau_0)^{-1-m\bar{L}C_1\sigma^\beta}$$

From eq. (2.53), it follows that the non-fracture probability leads to an infinite value for time t when the value a is larger than unity. The non-fracture probability is shown in Fig. 2.4.

The non-fracture probability at time $t=\infty$ is given by eq. (2.59):

$$\begin{aligned} P(t, \tau_0)_{t=\infty} &= \exp\left\{\frac{m\bar{L}C_1\sigma^\beta}{1-a}\tau_0^{1-a}\right\} \\ &= \frac{1}{\exp\left\{\dfrac{m\bar{L}C_1\sigma^\beta}{(a-1)\tau_0^{a-1}}\right\}} \end{aligned} \tag{2.59}$$

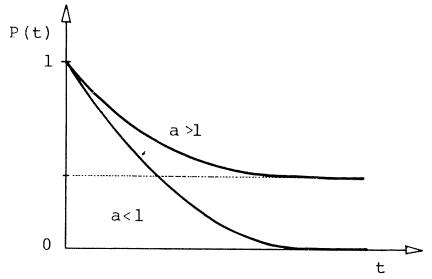

Fig. 2.4. Non-fracture probability under sustained load.

From equation (2.50) and eq. (2.57), the relationship between $\bar{t}$ and the static strength can be obtained as follows ($\eta = \sigma/\bar{\sigma}$):

$$\bar{t} = \frac{a}{(m\bar{L}C_1)^2}\left(\frac{m\bar{L}C_1}{\beta\dot{\sigma}}\right)^{\frac{2\beta}{\beta+1}} \tau_0^{\left(\frac{2a}{\beta+1}-1\right)}$$

$$\left\{(1/\eta)^{\beta} + \frac{m\bar{L}C_1\tau_0^{\left(1-\frac{a}{\beta+1}\right)}}{2a}\left(\frac{\beta\dot{\sigma}}{m\bar{L}C_1}\right)^{\frac{\beta}{\beta+1}}\right\}^2 - \frac{\tau_0}{4a} \tag{2.60}$$

$$= \frac{A1}{\tau_0^{\left(1-\frac{2a}{\beta+1}\right)}}\left\{(1/\eta)^{\beta} + A2\cdot\tau_0^{\left(1-\frac{a}{\beta+1}\right)}\right\}^2 - \frac{\tau_0}{4a}$$

This may be looked upon as being a deformated equation of eq. (2.61). (Fig. 2.5).

$$\bar{t} = \frac{A1}{\tau_0^{\left(1-\frac{2a}{\beta+1}\right)}}(1/\eta^{\beta})^2 \tag{2.61}$$

From eq. (2.60) it follows:

$$\bar{t} = \frac{1}{m\bar{L}C_1}\left(\frac{m\bar{L}C_1}{\beta\dot{\sigma}}\right)^{\frac{\beta}{\beta+1}}\left\{(1/\eta^{\beta})\tau_0^{\frac{a}{\beta+1}} + \frac{a}{m\bar{L}C_1}\cdot\left(\frac{m\bar{L}C_1}{\beta\dot{\sigma}}\right)^{\frac{\beta}{\beta+1}}\frac{1}{\tau_0^{1-\frac{2a}{\beta+1}}}(1/\eta^{\beta})^2\right\} \tag{2.62}$$

In the case of old specimens, the following equation may be useful.

$$\bar{t} = \frac{1}{m\bar{L}C_1}\left(\frac{m\bar{L}C_1}{\beta\dot{\sigma}}\right)^{\frac{\beta}{\beta+1}}\tau_0^{\frac{a}{\beta+1}}(1/\eta)^{\beta}$$

$$= \left\{\frac{\tau_0^a}{m\bar{L}C_1(\beta\dot{\sigma})^{\beta}}\right\}^{\frac{1}{\beta+1}}(1/\eta)^{\beta} \tag{2.63}$$

From eq. (2.45) and eq. (2.62), the following equation may be obtained for the model of type B.

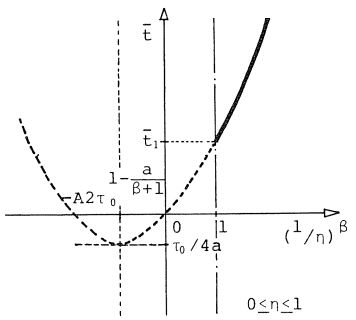

Fig. 2.5. Graphical representation of eq. (2.60).

$$\bar{t}=\frac{1}{m\bar{L}C_1}\cdot\left(\frac{m\bar{L}C_1}{\beta\dot{\sigma}}\right)^{\frac{\beta}{\beta+1}}\left\{\frac{1}{\eta^{\beta}}\cdot\tau_0^{\frac{a}{\beta+1}}\right.$$
$$\left.+\frac{a}{m\bar{L}C_1}\left(\frac{m\bar{L}C_1}{\beta\dot{\sigma}}\right)^{\frac{\beta}{\beta+1}}\frac{1}{\tau_0^{\left(1-\frac{2a}{\beta+1}\right)}}(1/\eta^{\beta})^2\right\}F(\lambda_1, m) \tag{2.64}$$

In the case of the loading condition as shown in Fig. 2.6, the non-fracture probability should be evaluated by eq. (2.65).

$$P(t)=\exp\left(-\int_0^t mL\sigma^{\beta}\cdot\mathrm{d}t\right)\cdot P(\sigma)$$
$$=\exp\left(-mL\sigma^{\beta}t\right)\exp\left\{-\frac{mL}{(\beta+1)\dot{\sigma}}\sigma^{\beta+1}\right\} \tag{2.65}$$

where $P(\sigma)$ means the non-fracture probability at point 1 in Fig. 2.6. Hence the following equation is obtained.

$$\bar{t}=\frac{1}{mL\sigma^{\beta}}\cdot\exp\left\{-\frac{mL}{(\beta+1)\dot{\sigma}}\cdot\sigma^{\beta+1}\right\} \tag{2.66}$$

Because of the same reason, eq. (2.64) may be rewritten as follows.

$$\bar{t}=\frac{1}{m\bar{L}C_1}\left(\frac{m\bar{L}C_1}{\beta\dot{\sigma}}\right)^{\frac{\beta}{\beta+1}}\left\{\tau_0^{\frac{a}{\beta+1}}\frac{1}{\eta^{\beta}}\right.$$
$$\left.+\frac{a}{m\bar{L}C_1}\left(\frac{m\bar{L}C_1}{\beta\dot{\sigma}}\right)^{\frac{\beta}{\beta+1}}\frac{1}{\tau_0^{1-\frac{2a}{\beta+1}}}\left(\frac{1}{\eta^{\beta}}\right)^2\right\}\exp\left\{-\frac{\beta}{\beta+1}\eta^{\beta+1}\right\}F(\lambda_1, m) \tag{2.67}$$

This equation will later be compared with published experimental data.

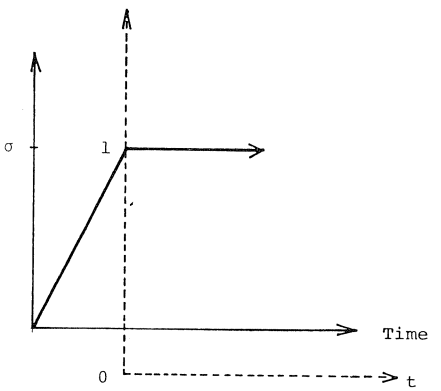

Fig. 2.6. Usual loading history for an experiment to determine the lifetime of a specimen.

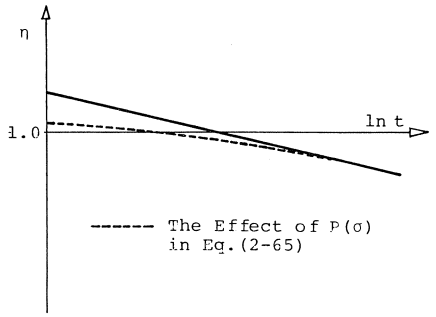

Fig. 2.7. Modified relationship.

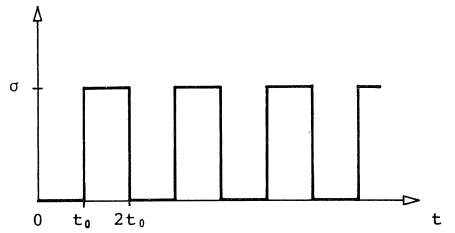

Fig. 2.8. Rectangular pulse loading condition.

2.4 *Strength under repeated load*

2.4.1 Fracture under repeated tensile or bending load

2.4.1.1 Rectangular pulse loading history

To begin with the description of fatigue of concrete, the simplest model (type A) will be used to study the failure process. A rectangular pulse loading history is being assumed. Then the non-fracture probability after one cycle of loading as shown in Fig. 2.8, is given by eq. (2.68):

$$P(1) = \exp\left\{-\int_0^{t_0} mL\sigma^{\beta} \cdot \mathrm{d}t\right\} \tag{2.68}$$

After N cycles of loading, the following equation expresses the non-fracture probability:

$$P(N) = \exp\left(-NmL\sigma^{\beta} t_0\right) \tag{2.69}$$

The probability density of the number of cycles N which leads to failure is given by eq. (2.70):

$$q(N) = mLt_0\sigma^{\beta} \cdot \exp\left(-mLNt_0\sigma^{\beta}\right) \tag{2.70}$$

The mean value of fatigue life is then described as follows:

$$\begin{aligned} \bar{N}_1 &= \frac{1}{mLt_0\sigma^{\beta}} \cdot \Gamma(2) \\ &= \frac{2f}{mL\sigma^{\beta}} \Gamma(2) \end{aligned} \tag{2.71}$$

where

$$f = \frac{1}{2t_0}$$

is the frequency of the cyclic loding history.

If we introduce

$$\bar{\sigma}_m = \left(\frac{\beta\dot{\sigma}}{mL}\right)^{\frac{1}{\beta+1}}$$

as the mean value of static strength as indicated by eq. (2.16) we can rewrite eq. (2.71) and obtain:

$$\ln \bar{N}_1 = -\beta \cdot \ln \eta + \ln \frac{2f}{mL} \cdot \left(\frac{mL}{\beta\dot{\sigma}}\right)^{\frac{\beta}{\beta+1}} \tag{2.72}$$

where $\eta = \sigma/\bar{\sigma}_m$

2.4.1.2 Triangular pulse loading history

Non-fracture probability after half-cycle of load history as shown in Fig. 2.9, is given by eq. (2.73).

$$P\left(\tfrac{1}{2}\right) = \exp\left\{-\frac{mL\dot{\sigma}^{\beta}}{\beta+1}\, t_0^{\beta+1}\right\} \tag{2.73}$$

If we suppose that the transient probability is dependent only on stress, the non-fracture probability after N cycles is described by eq. (2.74).

$$P(N) = \exp\left(-\frac{2NmL\sigma^{\beta}}{\beta+1}\, t_0\right) \tag{2.74}$$

The probability density $q(N)$ and the mean value of fatigue life $\bar{N}_2$ are given by eq. (2.75) and (2.76) respectively:

$$q(N) = \frac{2mL\sigma^{\beta}t_0}{\beta+1} \cdot \exp\left(-\frac{2mL\sigma^{\beta}t_0}{\beta+1} \cdot N\right) \tag{2.75}$$

$$\bar{N}_2 = \frac{(\beta+1)}{mL\sigma^{\beta}} f \tag{2.76}$$

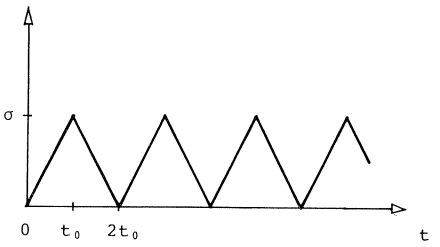

Fig. 2.9. Triangular pulse loading condition.

If we introduce again $\bar{\sigma}_m$ as the the mean value of static strength, the following equation is obtained:

$$\ln \bar{N}_2 = -\beta \ln \eta + \ln \frac{(\beta+1)\cdot f}{mL} \left(\frac{mL}{\beta \dot{\sigma}}\right)^{\frac{\beta}{\beta+1}} \tag{2.77}$$

as usual η stands for $\sigma/\bar{\sigma}_m$.

2.4.1.3 Sine-wave loading history

For experimental studies very often sine-wave loading history is chosen. In this case the non-fracture probability is given by the following equation:

$$P(1) = \exp\left\{-\int_0^{1/f} mL \cdot (\sigma_m + \sigma_a \cdot \sin 2\pi f t)^{\beta} \cdot \mathrm{d}t\right\} \tag{2.78}$$

Unfortunately it is very difficult to find an analytical solution of this equation. But the upper limit and the lower limit of $\bar{N}_3$, the fatigue life under cyclic loading, may be estimated by the results of 2.4.1.1 and 2.4.1.2:

$$\bar{N}_1 \leq \bar{N}_3 \leq \bar{N}_2 \tag{2.79}$$

From eq. (2.72) and eq. (2.77), the following relation is predicted between the fatigue life $\bar{N}$ and the upper bound stress level η for all kinds of constant amplitude loading condition.

$$\ln \bar{N} = -\beta \cdot \ln \eta + \text{constant} \tag{2.80}$$

where the constant is dependent on the chosen loading history.

2.4.2 Fracture under repeated compressive load

2.4.2.1 Rectangular pulse loading history

According to the model of type B, the following non-fracture probability and the mean value of fatigue life are obtained if rectangular pulse loading history is assumed:

$$P(N) = \frac{L_1^m}{(L_1 - L_0)^m} \cdot \exp\left(-mL_0\sigma^{\beta} t_0 N\right) \cdot \left[1 - \frac{L_0}{L_1} \exp\left\{(L_0 - L_1)\cdot \sigma^{\beta} \cdot t_0 N\right\}\right]^m \tag{2.81}$$

$$\bar{N} = \frac{1}{m^2 \sigma^{\beta} \cdot L_0 t_0}\left[\frac{L_1}{L_0}\cdot \Gamma(3) + \frac{L_1 \cdot (2mL_0 - L_1 - L_0)}{2mL_0^2}\cdot \Gamma(4) + \frac{\{L_1^2 + (1-3m)\cdot L_1 L_0 + m^2 L_0^2\}}{6mL_0^2}\cdot \Gamma(5)\right] \tag{2.82}$$

2.4.2.2 Triangular pulse loading history

The corresponding equations for non-fracture probability $P(N)$ and the mean life-time

under triangular loading history are found to be:

$$P(N) = \frac{L_1^m}{(L_1 - L_0)^m} \cdot \exp\left(-\frac{2mL_0\sigma^\beta t_0}{\beta+1} N\right) \cdot \left[1 - \frac{L_0}{L_1} \exp\left\{\frac{2(L_0 - L_1)}{(\beta+1)} \sigma^\beta t_0 N\right\}\right]^m \tag{2.83}$$

$$\bar{N} = \frac{(\beta+1)}{2m^2 L_0 t_0 \sigma^\beta}\left[\frac{L_1}{L_0}\Gamma(3) + \frac{L_1 \cdot (2mL_0 - L_1 - L_0)}{2mL_0^2}\Gamma(4) + \frac{\{L_1^2 + (1-3m)L_1 L_0 + m^2 L_0^2\}}{6mL_0^2} \cdot \Gamma(5)\right] \tag{2.84}$$

From eq. (2.82) and (2.84), the general relation between the upper stress and the fatigue life under compressive load may be expressed by eq. (2.80).

2.4.3 The influence of time-dependent deformation on fatigue life

Under repeated loading condition, an influence of time-dependent deformation on fatigue life cannot be excluded. Possible mechanisms to cause the change of internal structure include:

1. Increase of the radius of micro crack tip caused by creep deformation.
2. Stress redistribution caused by many stable cracks as discussed above.

The non-fracture probability of an element under rectangular loading conditions as shown in Fig. 2.11, is given by eq. (2.85).

$$\overset{e}{P}(N) = \exp\left\{-\int_0^N L \cdot (R^\beta + 1) \cdot \sigma^\beta \cdot t_0 \cdot dN\right\} \tag{2.85}$$

If we consider the change of internal structure under a certain sustained load, the following relation an be assumed:

$$\overset{e}{P}(N) = \exp\left\{-\int_0^N \frac{L \cdot (R^\beta + 1) \cdot \sigma^\beta \cdot t_0}{a \cdot (bS^\alpha N + 1)^r} dN\right\} \tag{2.86}$$

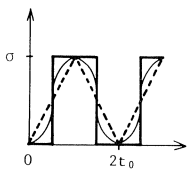

Fig. 2.10. Sine wave loading condition.

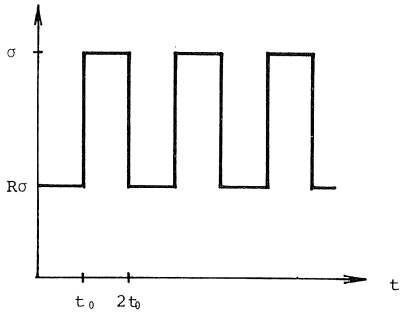

Fig. 2.11. Rectangular pulse loading condition superimposed to a constant load $R\sigma$.

where

$$S=\int_0^{2t_0}\{\sigma(t)\}^{\alpha 1}\cdot \mathrm{d}t=(R^{\alpha 1}+1)\cdot\sigma^{\alpha 1}\cdot t_0$$

and α may be a kind of materials parameter affected by temperature, humidity and the frequency of repeating load.

Hence the non-fracture probability of the specimen is obtained.

$$P(N)=\exp\left\{\frac{mL\cdot(R^{\beta}+1)\cdot\sigma^{\beta}\cdot t_0}{a\cdot b\cdot S^{\alpha}\cdot(1-r)}\right\}\cdot\exp\left\{-\frac{mL(R^{\beta}+1)\cdot\sigma^{\beta}t_0}{ab\cdot S^{\alpha}\cdot(1-r)}(bS^{\alpha}N+1)^{1-r}\right\} \tag{2.87}$$

and the probability density of fatigue life $q(N)$ is:

$$q(N)=\exp(A)\cdot A\cdot(1-r)bS^{\alpha}\cdot(bS^{\alpha}\cdot N+1)^{-r}\exp\{-A(bS^{\alpha}\cdot N+1)^{1-r}\} \tag{2.88}$$

where

$$A=\frac{mL\cdot(R^{\beta}+1)\cdot\sigma^{\beta}\cdot t_0}{abS^{\alpha}\cdot(1-r)}$$

The mean value of fatigue life is given by eq. (2.89).

$$\bar{N}=\frac{1}{bS}\cdot\exp\cdot(A)\cdot\left[\left(\frac{1}{A}\right)^{\frac{1}{1-r}}\cdot\Gamma\left(\frac{2-r}{1-r},A\right)-\Gamma(1,A)\right] \tag{2.89}$$

where

$$\Gamma\left(\frac{2-r}{1-r},A\right)$$

is the incomplete gamma function.

After asymptotic expansion, the following equation is obtained.

$$\bar{N}=\frac{a}{mLt_0\cdot(R^{\beta}+1)\cdot\sigma^{\beta}}\left[1+\frac{abr\cdot t_0^{\alpha}\cdot(R^{\alpha 1}+1)^{\alpha}\cdot\sigma^{\alpha 2}}{mL(R^{\beta}+1)\cdot\sigma^{\beta}\cdot t_0}+\frac{a^2b^2\cdot r\cdot(2r-1)\cdot t_0^{2\alpha}\cdot(R^{\alpha 1}+1)^{2\alpha}\cdot\sigma^{2\alpha 2}}{m^2L^2(R^{\beta}+1)^2\cdot\sigma^{2\beta}\cdot t_0^2}\right] \tag{2.90}$$

where $\alpha_2=\alpha_1\cdot\alpha$.

3 Comparison with published data

3.1 *Influence of rate of loading on strength*

The influence of rate of loading may be described by the following equation (see eq. 2.15) as shown above:

$$\frac{\bar{\sigma}}{\bar{\sigma}_0}=\left(\frac{\dot{\sigma}}{\dot{\sigma}_0}\right)^{\frac{1}{\beta+1}} \tag{3.1}$$

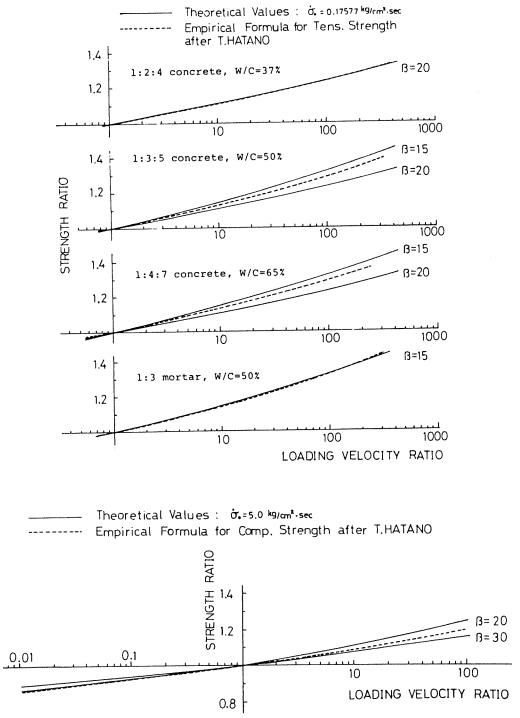

Fig. 3.1. Some empirical formulae of the influence of rate of loading compared with eq. (3.1).

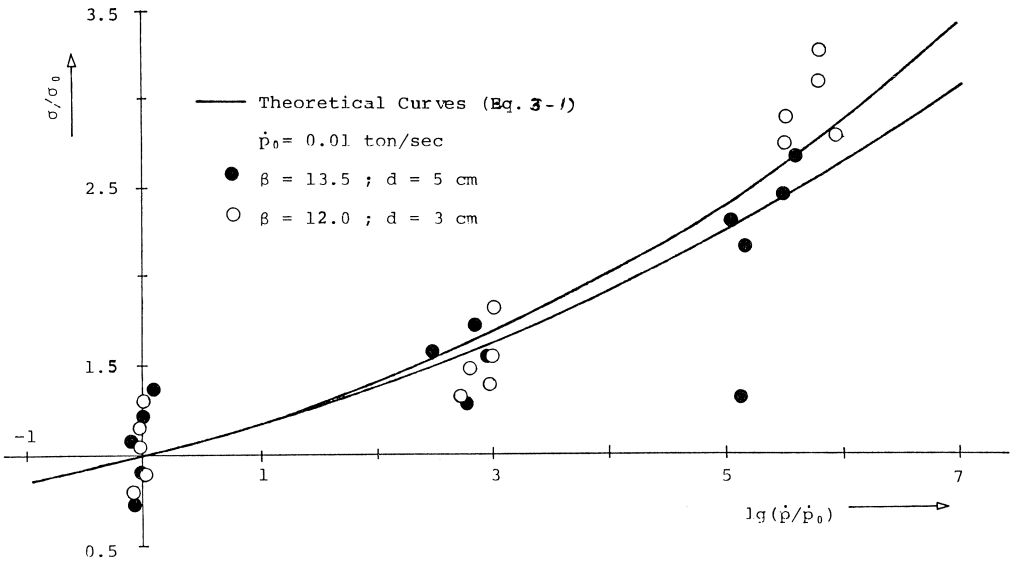

Fig. 3.2. Related flexural strength of concrete slab as function of related rate of loading (after J. Takeda).

$\bar{\sigma}$ and $\bar{\sigma}_0$ stand for strength under high rate of loading and for low rate of loading respectively. The corresponding rates of loading are called $\dot{\sigma}$ and $\dot{\sigma}_0$.

In Fig 3.1 and 3.2, some experimental results taken from Hatano [1961; 1968] and Takeda et al. [1976] are shown.

It is noteworthy that eq. (3.1) describes the dependence of strength under high rate of loading satisfactorily in a very wide range of different rates. This has been shown by other authors too in the mean-time [Zech and Wittmann 1980; Chandon et al. 1978].

3.2 *Aging effect and strength under sustained load*

If the load is kept constant on a level slightly below the critical load, the overall crack length increases as a function of the duration of load t.

Wittmann and Zaitsev [1973] obained the following theoretical expression after a mathematical treatment of this problem on the basis of crack propagation:

$$\eta = \frac{\sigma(t)}{\bar{\sigma}(\tau_0)} \sqrt{\frac{E(\tau_0)}{E(t)} \frac{1}{1+\varphi(t,\tau_0)}} \tag{3.2}$$

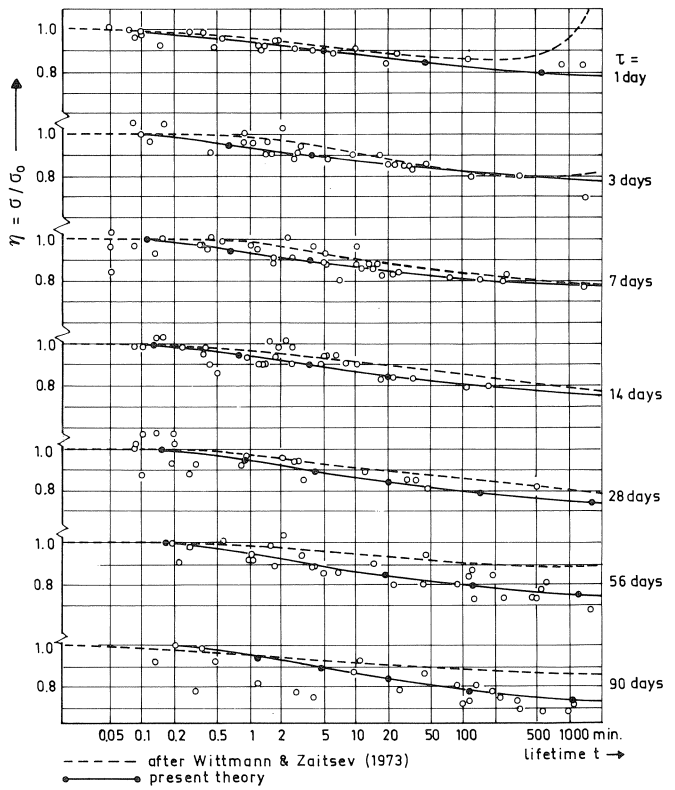

Fig. 3.3. Comparison of eq. (2.67) with experimental data of Wittmann and Zaitsev [1973] who determined the lifetime of hardened cement paste under sustained load.

where $\bar{\sigma}(\tau_0)$ and $E(\tau_0)$ are the strength and the Young's modulus respectively of the age of the specimen τ_0 at which the load has been applied. $\varphi(t, \tau_0)$ is the corresponding creep number.

In Fig. 3.3 and 3.4, a comparison of some experimental results with the theoretical equation (2.67) is presented. According to eq. (2.67), the following equations are obtained for Fig. 3.3 and 3.4 respectively:

$$\bar{t} = 0.03126 \left\{ \tau_0^{0.2344} \cdot (1/\eta)^{21.278} + \frac{66.484}{\tau_0^{0.5311}} \cdot (1/\eta)^{42.556} \right\} \exp\left(-0.9551 \cdot \eta^{22.278}\right) \tag{3.3}$$

$$\bar{t} = 0.00259 \left\{ \tau_0^{0.4344} \cdot (1/\eta)^{20.700} + \frac{40.826}{\tau_0^{0.1312}} \cdot (1/\eta)^{41.403} \right\} \exp\left(-0.9539 \cdot \eta^{21.70}\right) \tag{3.4}$$

Theoretical curves calculated with the help of eq. (3.2) are also shown in these figures.

It can be stated that there is good agreement between theoretical predictions and experimental findings within the range of accuracy of the measurements.

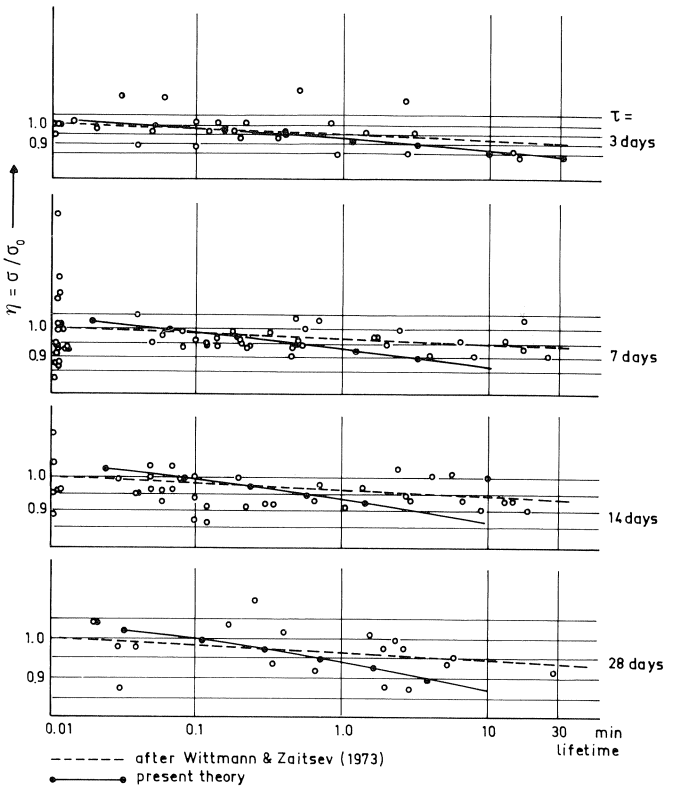

Fig. 3.4. Comparison of eq. (2.67) with experimental data of Wittmann and Zaitsev [1973] who determined the lifetime of concrete under high sustained load.

3.3 *Dynamic fatigue of concrete*

From eq. (2.87), the non-fracture probability after N cycles of loading, may be described as follows:

$$\ln\left(-\ln P(N)+Y_c\right)\simeq(1-r)\ln N+X_c \tag{3.5}$$

where $P(N)$ is non-fracture probability, r is parameter to introduce the effect of time-dependent deformation, X and Y are constants essentially affected by stress level and temperature. In Fig. 3.5, experimental results are compared with eq. (3.5).

According to eq. (2.90), the mean value of fatigue life (the number of load repetitions up to fracture) may be predicted by the following equation:

$$\bar{N}=\frac{2af}{mL(R^{\beta}+1)\sigma_u^{\beta}}\left\{1+\frac{abr(R^{\alpha 1}+1)^{\alpha}(2f)^{1-\alpha}}{mL(R^{\beta}+1)\sigma_u^{\beta-\alpha 2}}+\frac{a^2b^2\cdot r\cdot(2r-1)\cdot f^{2(1-\alpha)}\cdot(R^{\alpha 1}+1)^{2\alpha}}{m^2\cdot L^2\cdot(R^{\beta}+1)^2\cdot\sigma_u^{2(\beta-\alpha 2)}}\right\} \tag{3.6}$$

where f is frequency, R is σ_l/σ_u with σ_u and σ_l being upper and lower bound of the applied stress respectively, m is size factor of the specimen, β is a materials parameter, a, b, r, α and α_1 are parameters to introduce the effect of time-dependent deformation, α_2 is $\alpha_1\cdot\alpha$, L is a parameter representing the heterogeneity of internal structure. When the effect of time-dependent deformation is negligible, the relation between the mean value of fatigue life and the applied maximum stress may be described by the following linear equation:

$$\ln\bar{N}=-\beta\cdot\ln\sigma_u+F(m,L,R,f) \tag{3.7}$$

Fig. 3.6 shows the comparison of eq. (3.7) with the impact fatigue under direct tensile repeated loading. A good agreement between the experimental results and the theory is observed. Fatigue of concrete under compressive repeated load is also described satisfactorily by eq. (3.7) is shown in Fig. 3.7.

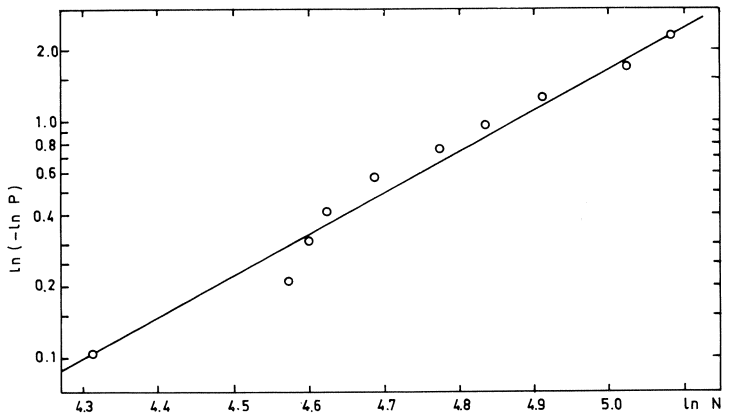

Fig. 3.5. Comparison of eq. (3.5) with experimental results (after Leeuwen and Siemes).

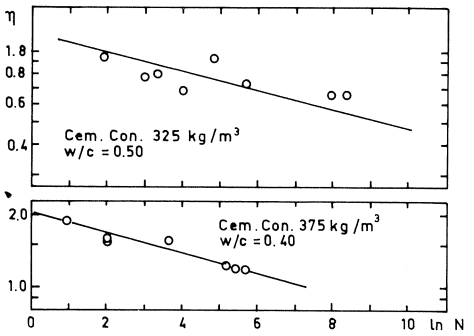

Fig. 3.6. Fatigue life under impact tensile load (after Reinhardt).

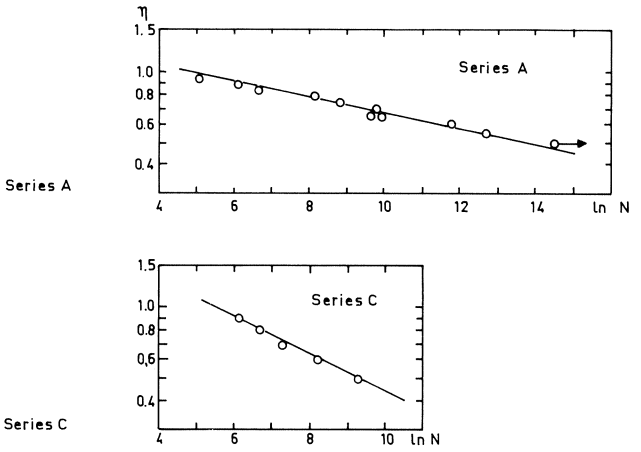

Fig. 3.7. Fatigue life under compressive load (after Leeuwen and Siemes).

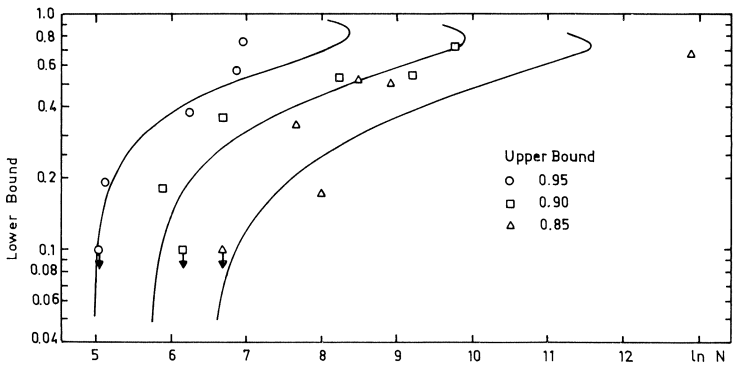

Fig. 3.8. Influence of the lower bound of the applied stress on fatigue life. Lines are calculated by using eq. (3.6) and experimental values are taken from a reference of Leeuwen and Siemes.

In Fig. 3.8 finally the influence of the lower bound of applied stress on the dynamic fatigue is presented. Theoretical curves calculated with the help of eq. (3.6) are shown for comparison.

4 Experiments and results

4.1 *General remarks on the experimental program*

Experiments were carried out with the aim to verify the theoretical approach described in this report. Two different series have been planed.

The materials tested and the corresponding loading conditions which were chosen in these programs are shown in tables 4.1 and 4.2. Ordinary Portland cement was used throughout the study (type B according to Dutch Standards). The age of the specimens at the time of testing was 28 days for all series.

In series I the influence of rate of loading on the mean strength and the variability was studied.

The rate of loading was changed by nearly three orders of magnitude. Several different rates were chosen within these ranges for each material. Specimens of high strength mortar, low strength mortar, ligth weight aggregate concrete and normal concrete were tested under uniaxial compressive load and in bending. About 30 individual tests were carried out for each chosen condition.

The influence of temperature was also investigated in series II. In this case the specimens were subjected to uniaxial compressive load. Two different environmental temperatures and two different rates of loading were chosen for each material.

Table 4.1 Experimental program to study the influence of rate of loading on mean strength and on variability of strength of concrete (series I).

group	material	loading condition	different rates of loading	number of tests
A	mortar (w/c = 0,45)	bending	5	148
B	mortar (w/c = 0,65)	bending	5	149
C	mortar (w/c = 0,45)	compression	6	188
D	mortar (w/c = 0,65)	compression	6	190
E	light weight concrete	bending	5	150
F	light weight concrete	compression	5	150
G	normal concrete	compression	2	60

Table 4.2 Experimental program to study the influence of temperature on strength of concrete (series II).

group	material	different temperatures	different rates of loading	number of tests
H	mortar (w/c = 0,45)	2	2	6
I	mortar (w/c = 0,65)	2	2	6
J	light weight concrete	2	2	6

4.2 *Experiments with mortar*

4.2.1 Experimental procedure

As indicated in Table 4.1 mortar prisms (40 mm × 40 mm × 160 mm) have been subjected to bending load and compressive load. The composition of the two types of mortar which have been tested in given in Table 4.3.

Steel moulds were filled with mortar and compacted with a table vibrator for five seconds.

Specimens were kept under moist cloth and demoulded next day. Then they were kept in water until the night before testing. Before loading, they were exposed to laboratory climatic conditions (20 °C, 60% RH) for about 16 hours.

The bending tests were performed on a displacement controlled loading device (Instron). A three-point-test was carried out and the beams were simply supported with a 100 mm span. The load was recorded by means of a conventional load cell.

The compression test was carried out in a 600 kN servo-hydraulic testing machine (Schenck). The load-displacement diagrams of three specimens were obtained for each rate of loading by means of strain gages. This was mainly done to check the influence of creep deformation. In the case of compression test, the displacement between loading plates was also recorded on a $X-Y$ recorder (HP: 7004 B). The rates of loading chosen for each loading condition are given in Table 4.4. For the bending tests the speed of the crosshead is indicated.

Table 4.3 Composition of the two types of mortar. The weight used for one batch is indicated.

Portland cement B:		450,0 g
water	w/c = 0,45:	202,5 g
	w/c = 0,65:	292,5 g
river sand	2,0 ~ 4,0 mm:	67,5 g
	1,0 ~ 2,0 mm:	378,0 g
	0,5 ~ 1,0 mm:	459,0 g
	0,25 ~ 0,5 mm:	310,5 g
	0,125 ~ 0,25 mm:	135,0 g
	total:	1350,0 g

Table 4.4 Different rates of loading chosen for the tests on mortar specimens.

	bending test A: w/c = 0,45 B: w/c = 0,65	compressive load C: w/c = 0,45 D: w/c = 0,65
1	20,0 mm/min (3854,20 N/sec)	50,505 N/mm^2 · sec
2	10,0 mm/min (1944,10 N/sec)	25,253 N/mm^2 · sec
3	5,0 mm/min (1022,08 N/sec)	5,173 N/mm^2 · sec
4	1,0 mm/min (200,45 N/sec)	2,586 N/mm^2 · sec
5	0,1 mm/min (18,074 N/sec)	0,259 N/mm^2 · sec
6		0,052 N/mm^2 · sec

The values given in Table 4.4 in parentheses mean the approximate rate of loading calculated from the experimental results.

4.2.2 Results

The test results of the groups A to D are given in Tables 4.5 to 4.8. The standard deviation was calculated by using the following equation according to Bessel's correction:

$$V(\sigma) = \sqrt{\frac{\sum_{i}^{n} (\bar{\sigma} - \sigma_i)^2}{n-1}} \tag{4.1}$$

where $\bar{\sigma}$ is mean value of strength and n is the total number of individual tests.

Table 4.5 The relation between the rate of displacement and strength of mortar (w/c = 0,45) under bending loading condition (test group A).

rate of displacement (mm/min)	mean value of strength (N/mm^2)	standard deviation	coefficient of variation	value of β_S*
20,0	8,7203	0,67705	0,078	13,222
10,0	8,4766	0,71270	0,084	12,002
5,0	8,3887	0,68489	0,082	12,488
1,0	8,1136	0,58505	0,072	13,683
0,1	6,8668	0,72897	0,106	8,969

* The value of β_S was obtained according to eq. (2.13).

Table 4.6 The relation between the rate of displacement and strength or mortar (w/c = 0,65) under bending loading conditions (test group B).

rate of displacement (mm/min)	mean value of strength (N/mm^2)	standard deviation	coefficient of variation	value of β_S
20,0	8,4355	0,71630	0,085	11,746
10,0	7,9336	0,81962	0,103	8,896
5,0	8,1270	0,62945	0,077	12,872
1,0	7,4507	0,54210	0,073	14,069
0,1	6,2836	0,46496	0,074	13,758

Table 4.7 The relation between the rate of loading and strength of mortar (w/c = 0,45) under compressive load (test group C).

rate of loading ($N/mm^2 \cdot sec$)	mean value of strength (N/mm^2)	standard deviation	coefficient of variation
50,505	46,514	5,0749	0,109
25,253	43,366	6,3480	0,146
5,173	40,628	5,9925	0,147
2,586	41,298	5,8996	0,143
0,259	37,978	5,2945	0,139
0,052	35,517	3,9054	0,110

Table 4.8 The relation between the rate of loading and strength of mortar (w/c = 0,65) under compressive load (test group D).

rate of loading ($N/mm^2 \cdot sec$)	mean value of strength (N/mm^2)	standard deviation	coefficient of variation
50,505	33,152	4,6688	0,141
25,253	33,382	3,5767	0,107
5,173	30,629	3,0357	0,099
2,586	29,548	3,0142	0,102
0,259	26,862	3,9058	0,145
0,052	26,220	3,6890	0,141

Figs. 4.1 and 4.2 show the relation between the rate of loading and the mean value of strength under bending and compressive load respectively. By fitting the data with eq. (2.15), the following relations were obtained for the different series:

Group A:
(Bending test; mortar w/c = 0,45)

$$\ln \sigma = 0{,}043 \cdot \ln \dot{\delta} + 2{,}050$$
$$\beta_D = 22{,}2$$

Group B:
(Bending test; mortar w/c = 0,65)

$$\ln \sigma = 0{,}053 \cdot \ln \dot{\delta} + 1{,}980$$
$$\beta_D = 17{,}8$$

Group C:
(Compressive load; mortar w/c = 0,45)

$$\ln \sigma = 0{,}035 \cdot \ln \dot{\sigma} + 3{,}675$$
$$\beta_D = 27{,}4$$

Group D:
(Compressive load; mortar w/c = 0,65)

$$\ln \sigma = 0{,}038 \cdot \ln \dot{\sigma} + 3{,}361$$
$$\beta_D = 25{,}2$$

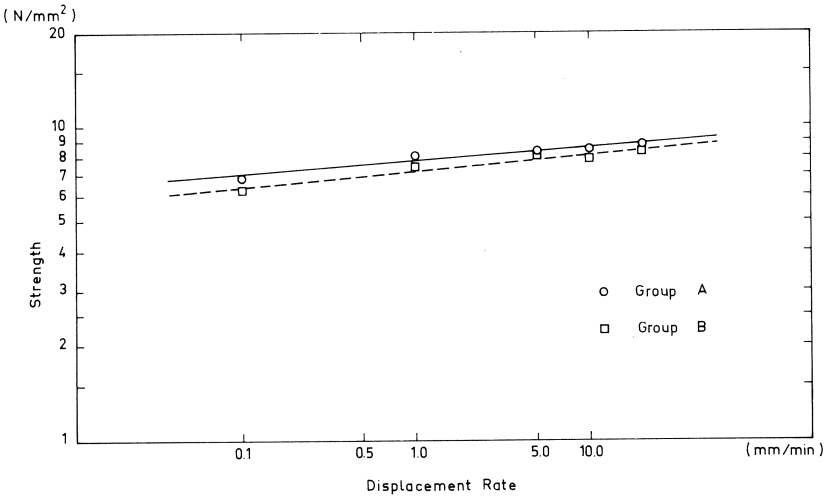

Fig. 4.1. Relation between the rate of loading and the mean value of flexural strength of mortar.

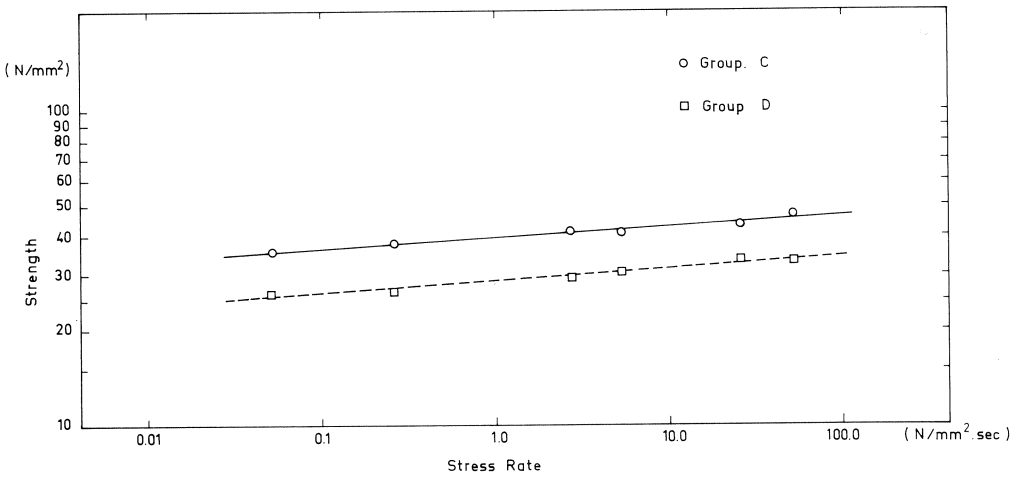

Fig. 4.2. Relation between the rate of loading and the mean value of compressive strength of mortar.

The value of β_D was obtained from the relation:

$$\ln \sigma = \frac{1}{(\beta_D + 1)} \ln \dot{\sigma} + \text{constant}$$

The probability of failure of mortar prisms (w/c = 0,45) under bending stress and compressive load is shown in Figs. 4.3 and 4.4 respectively. The probability of failure $D(\sigma)$ was calculated by dividing the rank of each specimen by $(n+1)$, where n equals the total number of specimens tested at this rate of loading.

The reason for dividing by $(n+1)$ rather than by n, is to avoid a probability of failure of 1.00 for the specimen having the highest σ-value.

The relation between Young's modulus (obtained from the displacement between loading plates) and compressive strength is given in Fig. 4.5. By linear regression the following equations are obtained:

Series C:

$$\ln \sigma = 0{,}952 \ln E - 5{,}843$$

Series D:

$$\ln \sigma = 0{,}567 \ln E - 2{,}130$$

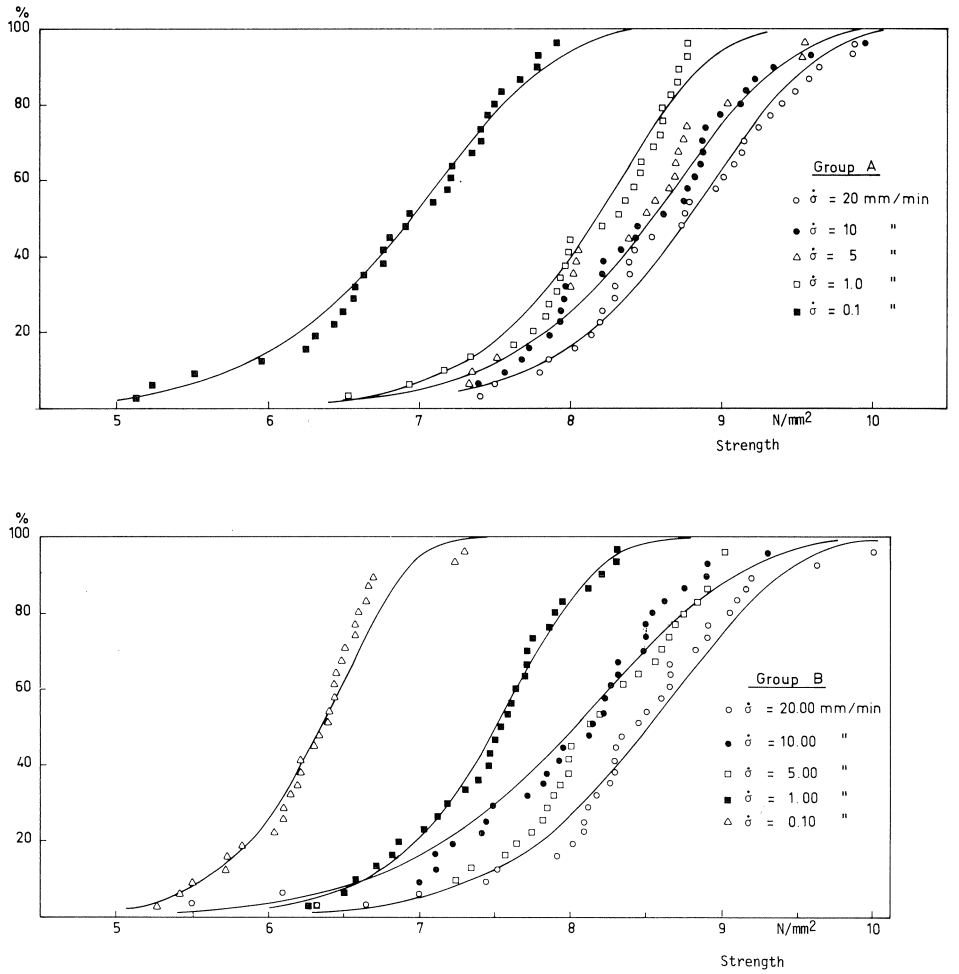

Fig. 4.3. Probability of failure of mortar under bending load. Group A (a) and group B (b) are plotted separately.

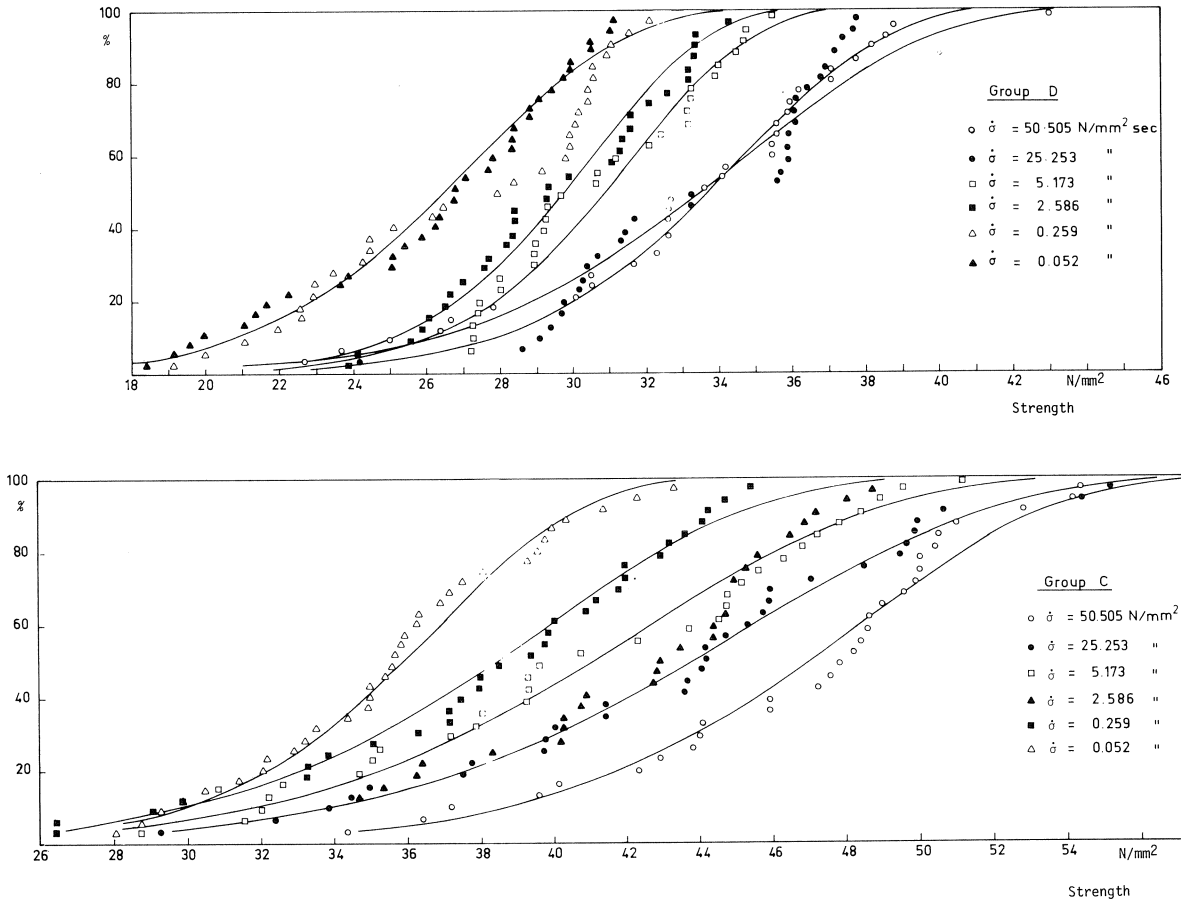

Fig. 4.4. Probability of failure of mortar under compressive load. Group C (a) and group D (b) are plotted separately.

4.3 *Experiments with light weight concrete*

4.3.1 Experimental procedure

For the tests with light weight concrete, prisms with the following dimensions have been prepared: 40 mm × 40 mm × 160 mm. Sixty prisms were cast at a time from one mix.

Natural river sand and Liapor light weight aggregates having a maximum size of about 8 mm were used. The water-cement ratio was 0,55. The light weight aggregates were put in water for several hours before mixing. Therefore the actual water-cement ratio might be increased some what. Details of mix proportions are indicated in Table 4.9.

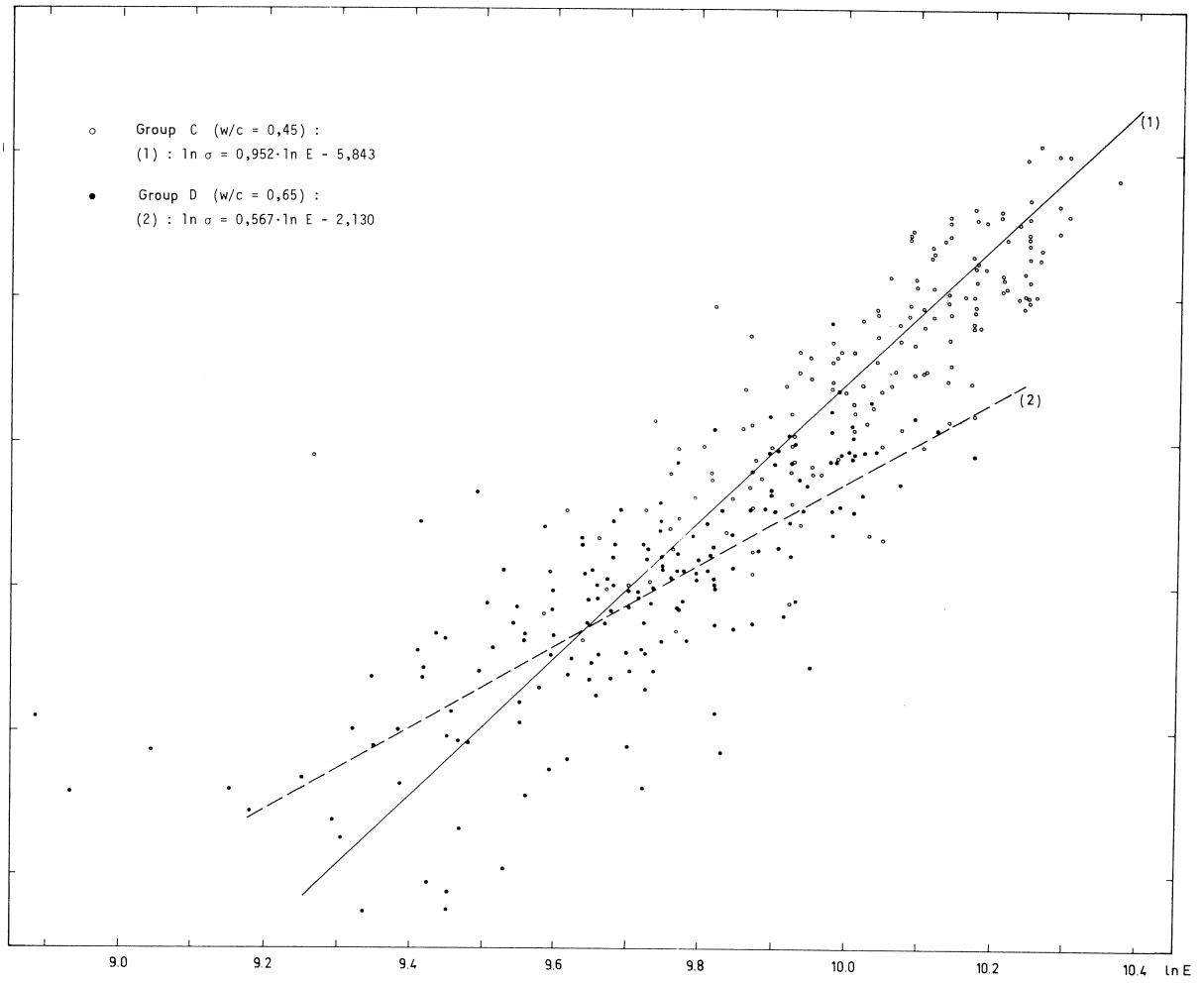

Fig. 4.5. Relation between Young's modulus and compressive strength.

Table 4.9 Composition of the light weight concrete. The indicated weights were mixed to prepare 60 specimens of 40 mm × 40 mm × 160 mm.

Portland cement A	5,400 kg
water	2,970 kg
river sand	9,300 kg
liapor (light weight aggregate)	9,075 kg
water taken up by liapor	1,972 kg

Typical sieve analyses of light weight aggregate and the sand are given in Table 4.10.

Table 4.10 Sieve analyses of light weight aggregate and river sand.

diameter (mm)	liapor (%)	river sand (%)
> 8	51	0,5
> 4	95,2	6,8
> 2	100,0	14,8
> 1	-	27,1
> 0,5	-	59,7
> 0,25	-	94,3
> 0,125	-	99,3
rest	-	100,0

Steel moulds were filled with fresh light weight concrete and compacted with a powerful table vibrator for 5 seconds. Next day all specimens were demoulded and cured in water for 27 days at 20 °C. They were only removed from the water immediately before the loading. The same loading machine as mentioned in the preceding section (groups A and B) was used for the bending tests. The compressive tests were again performed on a 600 kN servo-hydraulic testing machine (Schenck). In the case of compressive test the displacement (of the loading plate) has been recorded. The five different rates of loading which have been chosen for the two loading conditions are indicated in Table 4.11.

Table 4.11 Different rates of loading to determine strength of light weight concrete under bending and compressive load.

no.	bending load (group E)	compressive load (group F)
1	20,0 mm/min	50,505 $N/mm^2 \cdot sec$
2	10,0	25,253
3	5,0	5,173
4	1,0	0,517
5	0,1	0,052

4.3.2 Results

The test results of group E and F are shown in Table 3.12 and 3.13. Fig. 4.6 shows the relation between the rate of loading and the mean value of strength under bending and compressive load respectively. According to eq. (2.15), the following relations were obtained:

Group E:
(Bending)

$$\ln \sigma = 0{,}038 \cdot \ln \dot{\delta} + 1{,}441$$
$$\beta_D = 25{,}6289$$

Group F:
(Compression)

$$\ln \sigma = 0{,}017 \cdot \ln \dot{\sigma} + 2{,}566$$
$$\beta_D = 58{,}7533$$

Table 4.12 The relation between the rate of displacement and strength of light weight concrete under bending load (test group E).

rate of displacement (mm/min)	mean value of strength (N/mm^2)	standard deviation	coefficient of variation	value of β_S
20,0	4,6133	0,50005	0,108	9,113
10,0	4,5934	0,44372	0,097	10,237
5,0	4,6277	0,47012	0,102	9,828
1,0	4,2832	0,38221	0,089	11,335
0,1	3,8195	0,35094	0,092	10,827

Table 4.13 The relation between rate of loading and strength of light weight concrete under compressive load (test group F).

rate of loading ($N/mm^2 \cdot sec$)	mean value of strength (N/mm^2)	standard deviation	coefficient of variation
50,505	13,293	4,3456	0,327
25,253	13,793	3,0389	0,220
5,173	14,230	3,1460	0,221
0,517	12,838	2,7966	0,218
0,052	12,148	2,3532	0,194

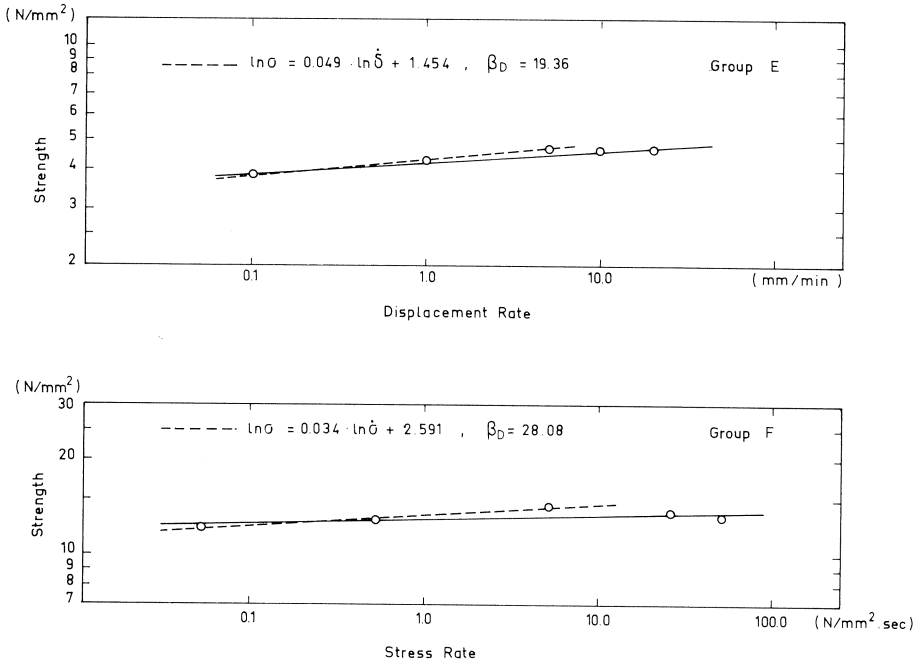

Fig. 4.6. Relation between the rate of loading and the mean value of flexural and compressive strength of light weight concrete.

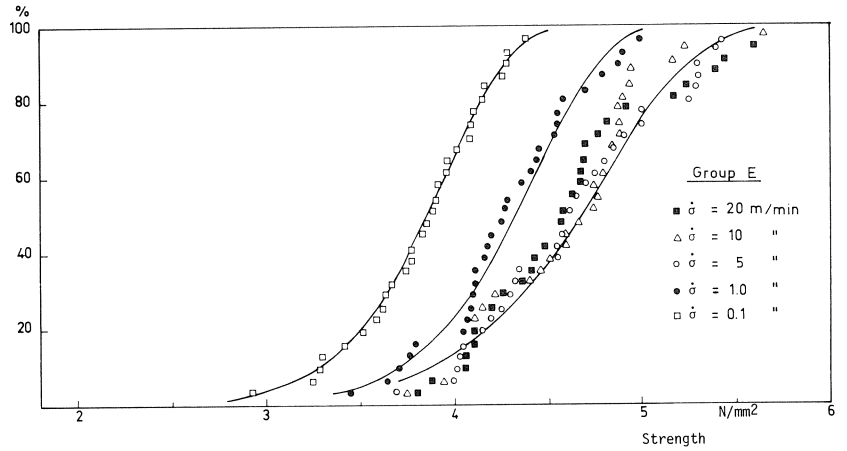

Fig. 4.7. Probability of failure of light weigth concrete under bending load.

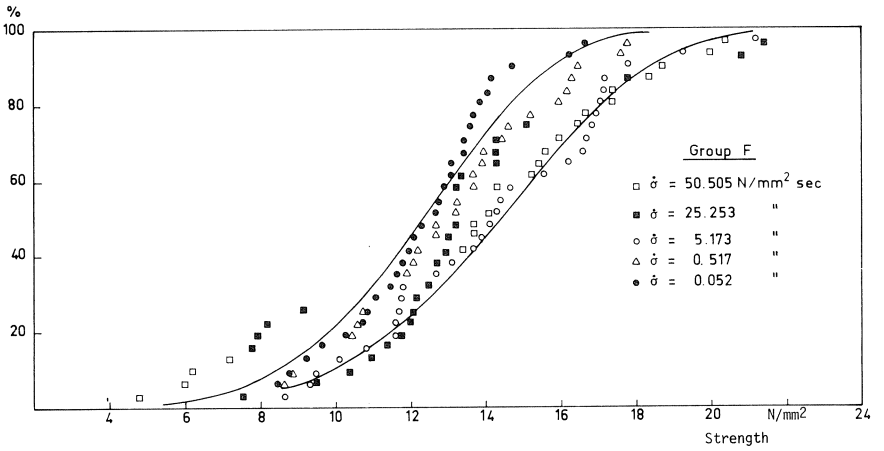

Fig. 4.8. Probability of failure of light weight concrete under compressive load.

The behaviour of light weight concrete under high rate of loading seems to be very different from that of other materials.

The probability of failure of light weight concrete under bending and compressive load are shown in Figs. 4.7 and 4.8 respectively.

4.4 *Experiments with normal concrete*

4.4.1 Experimental procedure

The prismatic specimens used for this study had a cross section of 100 mm × 100 mm and a length of 300 mm. Thirty test pieces were cast at a time from one mix. The same

natural river sand as mentioned in table 4.10 and rounded coarse aggregates (maximum grain size: 31,5 mm) were used. The water-cement ratio was 0,50 and a slump of 5,5 mm was measured. Details of the composition of the aggregates used are to be found in table 4.14.

Table 4.14 Sieve analyses of gravel and sand.

seive	gravel	sand
31,5 mm	1,0%	- %
16 mm	51,4%	- %
8 mm	88,4%	0,5 %
4 mm	98,4%	6,8 %
2 mm	99,8%	14,8 %
1 mm	99,8%	27,1 %
500 µm	100,0%	59,7 %
250 µm	- %	94,3 %
125 µm	- %	99,3 %
Rest	- %	(100,0)%

Table 4.15 Composition of one mix of normal concrete for 30 specimens.

Portland cement A	30,0 kg
water	15,0 kg
sand	74,7 kg
gravel	125,5 kg

The filling of the steel moulds was carried out in two equal layers.

Each layer was compacted seperately on a powerful vibrating table until the corners of the mould were filled with fresh concrete. Specimens were demoulded the following day and cured in a moist room for 27 days at 20 °C. Prior to testing two strain gages were glued on two opposite sides of every prism for strain measurement. The compressive tests were performed on a 600 kN Servo-hydraulic testing machine (Schenck). Two rates of loading were used with a difference of about three orders of magnitude. The fast one was 17,34100 $N/mm^2 \cdot sec$ and the slow one was 0,017932 $N/mm^2 \cdot sec$.

4.4.2 Results

The test results of the group G are shown in table 4.16.

Table 4.16 The relation between the rate of loading and strength of normal concrete under compressive load.

rate of loading ($N/mm^2 \cdot sec$)	mean value of strength (N/mm^2)	standard deviation	coefficient of variation
17,341	37,8615	2,80478	0,074
0,017932	29,3145	2,15095	0,073

There were no significant differences observed in the failure mode by comparing test of different rates of loading.

Fig. 4.9 shows the relation between the rate of loading and the mean value of strength.

This relation can be described as follows:

Group G:
(Compression)

$$\ln \sigma = 0{,}037 \cdot \ln \dot{\sigma} + 3{,}271$$
$$\beta_D = 25{,}8685$$

The probability of failure is shown in Fig. 4.10.

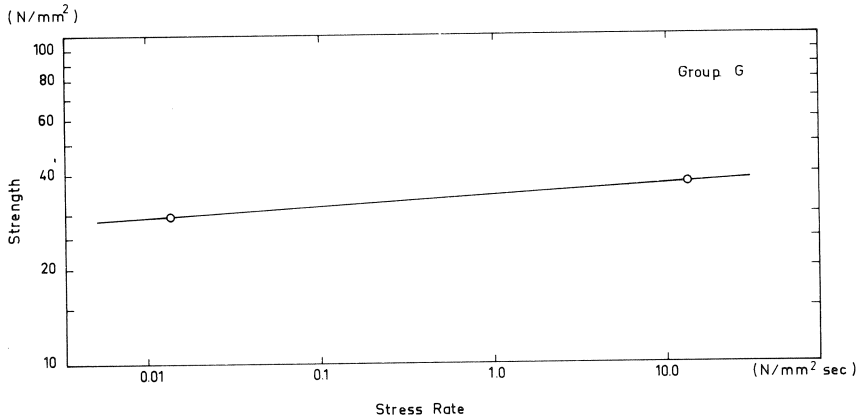

Fig. 4.9. Relation between the rate of loading and the mean value of compressive strength of normal concrete.

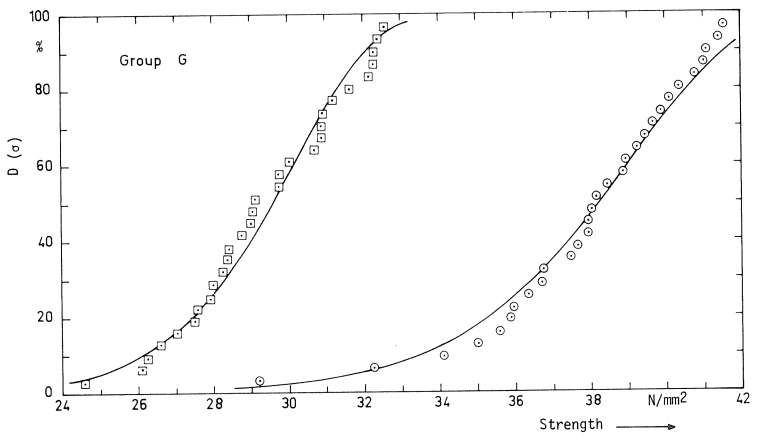

Fig. 4.10. Probability of failure of normal concrete under compressive load.

4.5 *Influence of temperature*

4.5.1 Experimental procedure

Prismatic specimens (40 mm × 40 mm × 160 mm) were subjected to compressive load. Three kinds of materials were used. The materials of group H (mortar: w/c = 0,45), I (mortar: w/c = 0,65) and J (light weight concrete) were prepared in the same way as those of corresponding groups C, D and F.

Two different temperature conditions were produced in a specially designed chamber, in which the specimens could be subjected to load.

The high temperature was + 80 °C and the low temperature was − 5 °C. Moreover, two rates of loading were chosen.

The fast rate of loading was 50,505 $N/mm^2 \cdot sec$ and the slow rate of loading was 0,052 $N/mm^2 \cdot sec$.

Before the loading, all specimens were put in the temperature chamber for several hours to reach thermal equilibrium. Three tests were carried out for each condition.

4.5.2 Results

The test results of the groups H to J are given in table 4.17. Fig. 4.11 shows the influence of environmental temperature on strength of mortar and light weight concrete. The results of 20 °C are taken from the other groups mentioned in previous sections. In the case of mortar, the strength is decreased by increasing temperature.

On the other hand, the strength of light weight concrete is not decreased significantly.

Table 4.17 Influence of temperature on strength. All individual values together with the mean value, in parentheses, are given.

	low temperature (−5 °C)		high temperature (80 °C)	
group	fast	slow	fast	slow
H	45,30 N/mm^2	42,30 N/mm^2	39,90 N/mm^2	28,05 N/mm^2
	46,17	41,25	38,07	32,55
	39,90	39,06	33,00	34,20
	(43,79)	(40,87)	(36,99)	(31,60)
I	41,46 N/mm^2	35,64 N/mm^2	24,45 N/mm^2	25,50 N/mm^2
	36,12	34,50	28,50	26,925
	39,09	32,55	22,50	26,91
	(38,89)	(34,23)	(25,15)	(26,445)
J	9,39 N/mm^2	10,20 N/mm^2	10,35 N/mm^2	9,75 N/mm^2
	10,575	9,075	8,025	12,72
	11,85	9,525	12,60	11,10
	(10,605)	(9,60)	(10,325)	(11,19)

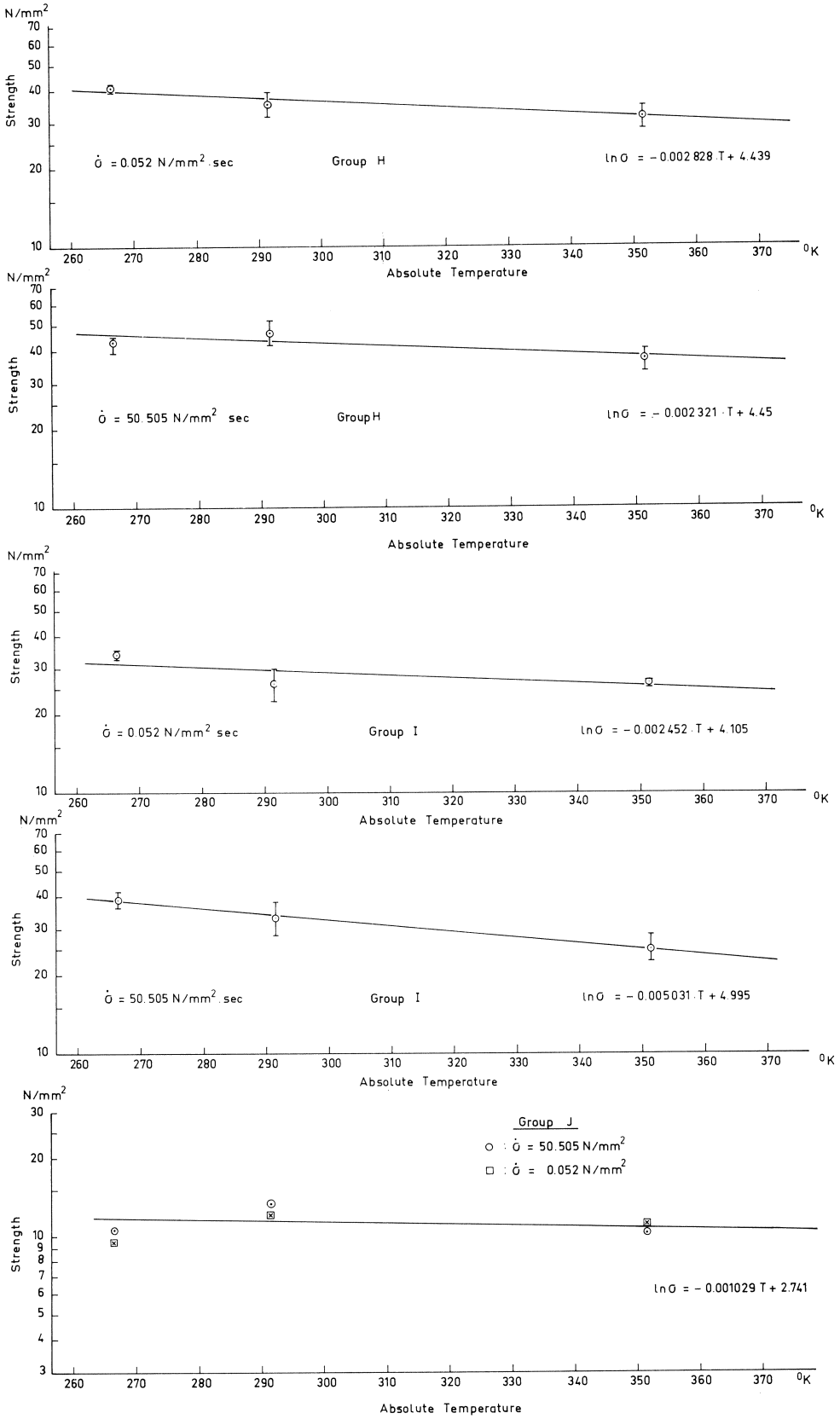

Fig. 4.11. Influence of environmental temperature on strength for group H (a), group I (b) and group J (c).

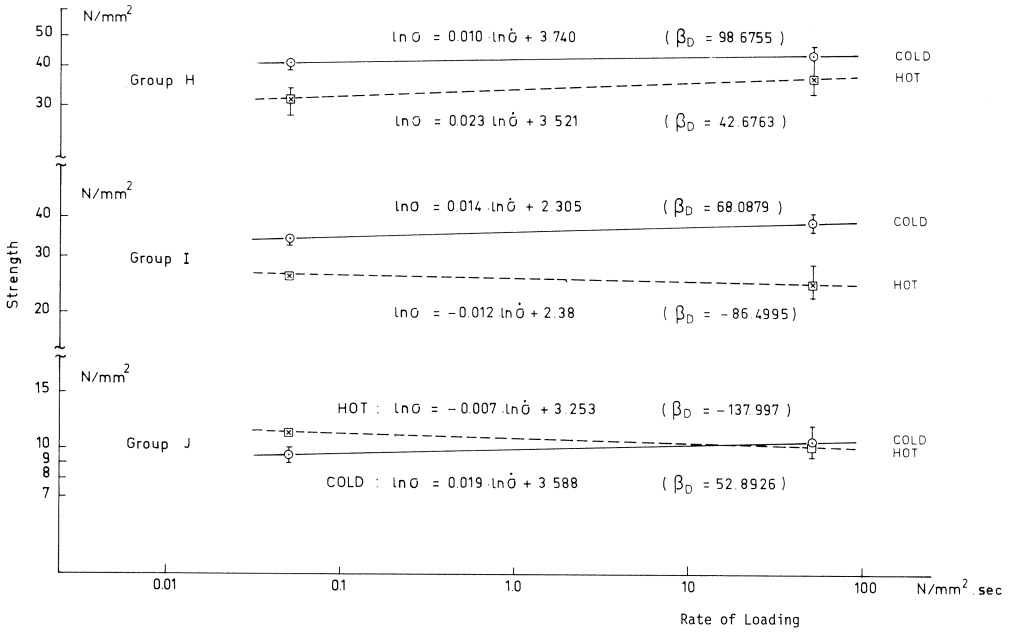

Fig. 4.12. Influence of rate of loading on strength at different temperatures.

Fig. 4.12 shows the influence of rate of loading on strength of different temperatures. The number of tests was not sufficient to provide a basis of the determination of values such as β.

5 Discussion

Influence of rate of loading on the mean value of strength

The theoretical prediction of eq. (2.15) satisfactorily agrees with the experimental results within the tested range of rate of loading as indicated by Figs. 4.1, 4.2 and 4.6. Figs. 5.1 and 5.2 show the relation between related strength and related rate of loading under bending and compressive load respectively. The following theoretical equation can be used to describe the influence of rate of loading on strength of composite aggregative materials from eq. (3.1):

$$\bar{\sigma}/\sigma_0 = (\dot{\sigma}/\dot{\sigma}_0)^{\frac{1}{\beta_D + 1}} \tag{5.1}$$

where $\bar{\sigma}_0$ and $\dot{\sigma}_0$ are reference mean value of strength and reference rate of loading respectively.

Table 5.1 gives the values of β_D which are experimentally obtained by means of eq. (5.1). High strength mortar gives comparatively low values of β. This tendency is in agreement with earlier results described by Reinhardt [1979] and Zech and Wittmann

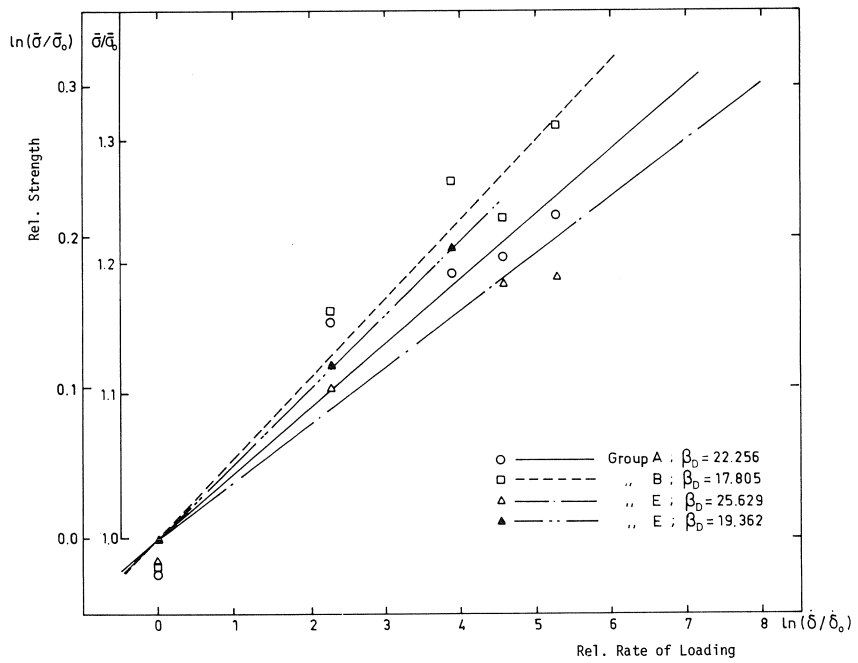

Fig. 5.1. Relation between the Related Rate of Loading and the Related Mean Value of Flexural Strength.

[1980]. For the same material the evaluation of compressive strength leads to higher values of β than those deduced from bending strength. Light weight concrete shows rather exceptional behaviour above $\dot{\sigma}/\dot{\sigma}_0 = 100$. This might be caused by the difference of failure mechanism. In the case of light weight concrete, failure is not only a process within hardened cement paste, but aggregates play an active role. *Their strength is comparable with the strength of the matrix. High strength concrete probably reacts in a similar way.*

Table 5.1 Compilation of values of β as determined in this project. β_D is obtained by applying eq. (5.1) and β_S is deduced from the probability of failure under bending load. Values given as (E') and (F') are evaluated by neglecting results of high rates of loading.

group	β_D	β_S
A	22,2	13,1
B	17,8	13,3
C	27,4	-
D	25,2	-
E	25,6	11,4
(E')	(19,3)	
F	58,7	-
(F')	(28,0)	
G	25,8	-

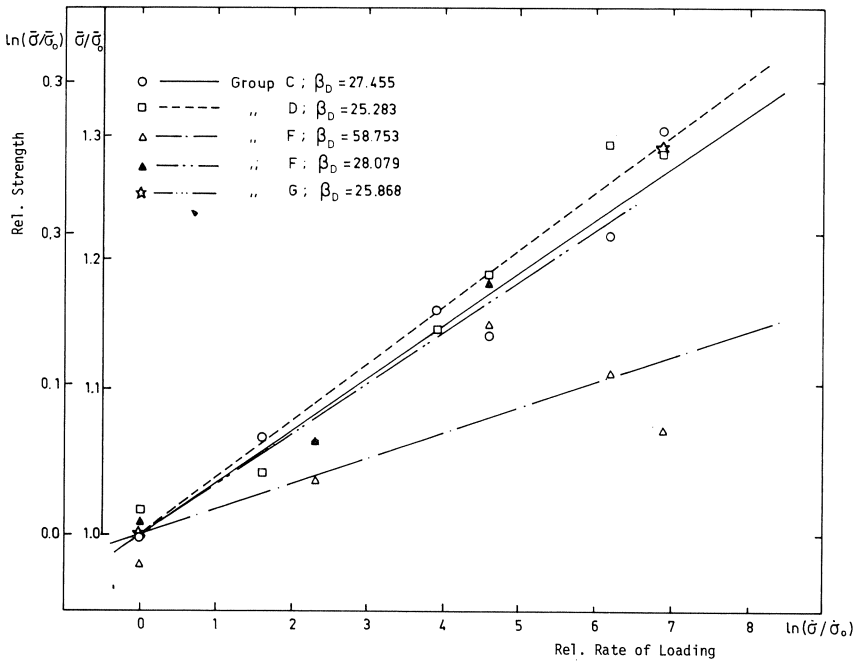

Fig. 5.2. Relation between the Related Rate of Loading and the Related Mean Value of Compressive Strength.

If we assume that high rate of loading stimulate preferably the failure of weak light weight aggregates, the strength of light weight concrete does not increase with increasing rate of loading as predicted by the theory. If we neglect for a moment the discrepancy in the region of high rates of loading, the theoretical equation can be applied in the region below $\dot{\sigma} = 10$ N/mm^2 · sec (compression). The corresponding values determined from data shown in Figs. 5.1 and 5.2 are designated by E′ and F′ in the figures and in Table 5.1 respectively.

Coefficient of variability

The theory predicts that the coefficient of variability is not influenced by rate of loading. The constance of the coefficient of variability is of major interest in connection with a realistic reliability assessment of a concrete structure. Within the range of accuracy, this theoretical prediction is verified by the present results. Table 5.2 gives the mean value of the coefficient of variability. High values of the coefficient of variability for light weight concrete under compressive load might be caused by the stiffness of the loading machine. The value of normal concrete may be looked upon to be reasonable for compressive strength.

Table 5.2 Compilation of coefficients of variability.

series	coefficients of variability
A	0,0844
B	0,0824
C	0,1323
D	0,1403
E	0,0976
F	0,2360
G	0,0735

Probability of failure

Since the coefficient of variability is not influenced by rate of loading, it is reasonable to expect that the distribution function of the strength, normalized by the mean value for each of loading, will be the same. Fig. 5.3, A to G, give the histograms for normalized strength and the theoretical density functions. Most of the results can be satisfactorily described by the Weibull distribution function (eq. 3.14). Group F only shows better agreement with a normal distribution function (Gaussian distribution).

Values of β

The parameter β plays a dominant role in the theoretical prediction. The exact value is highly dependent on the method used for the determination as well as on the material. Table 5.1 shows that the value of β obtained from the results of rate of loading (β_D) is higher than that obtained from the probability of failure (β_S). The reason for this discrepancy is not yet fully understood. This will be a matter of further investigation. The value of β for compressive strength is somewhat higher than the corresponding value for bending strength. This tendency is in accordance with results of previous studies [Zech and Wittmann, 1979].

Influence of environmental temperature

The stochastic theory on which this report is based and which is mentioned in chapter 2 predicts the invluence of environmental temperature as follows [Mihashi and Izumi, 1977]:

$$\ln \sigma = A \cdot T + B \tag{5.2}$$

where σ is the strength and T is the environmental absolute temperature; A and B are material constants which might be affected by testing conditions.

The present results, except group J (light weight concrete under high rate of loading) are in agreement with this theoretical prediction. In previous studies, A was found to be in the range of 0,0037 to 0,0061. The present results show slightly smaller values.

According to the theoretical prediction, the value of β is also affected by temperature. The relation between β and T is found to be:

$$\beta \propto \frac{1}{T} \tag{5.3}$$

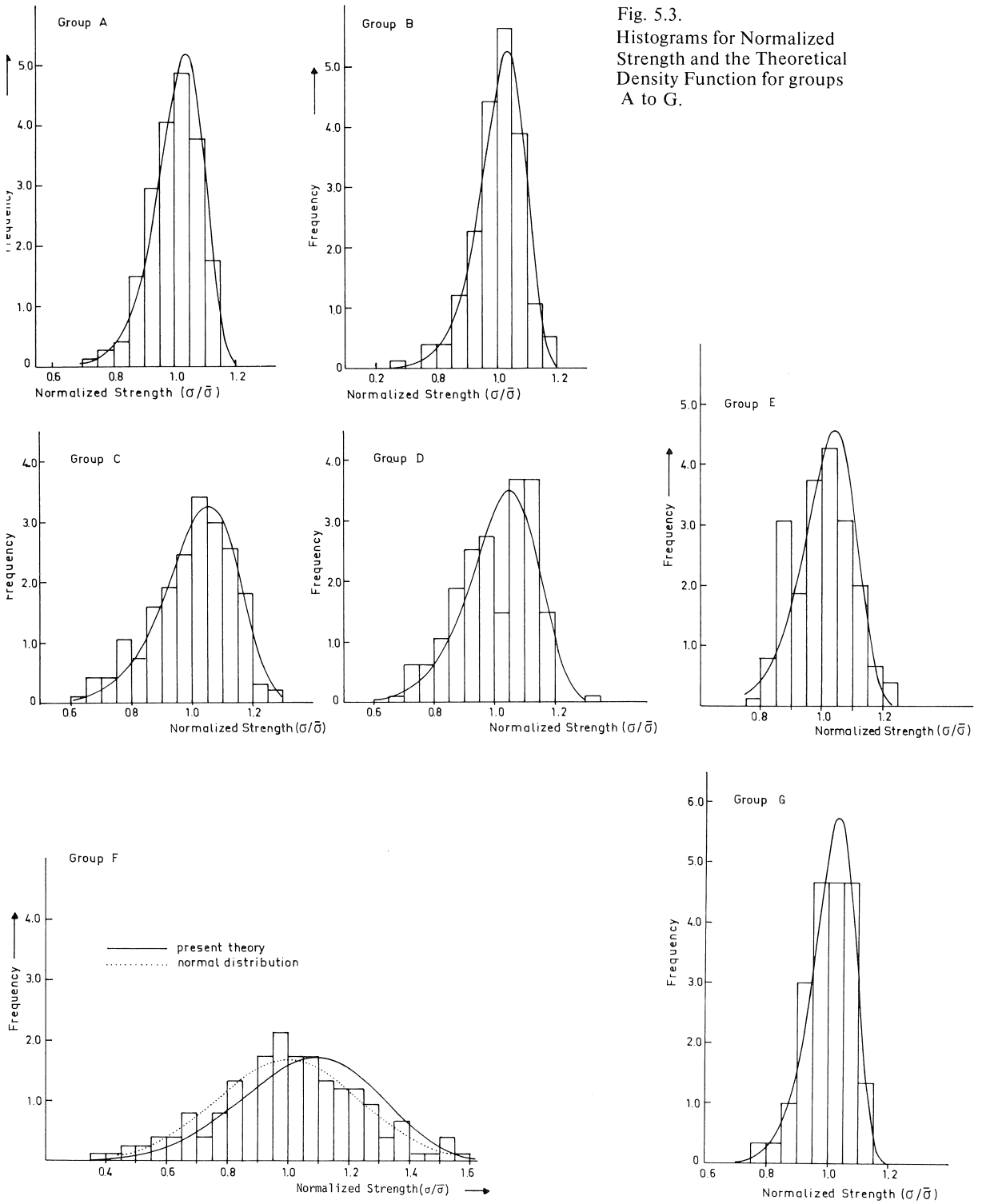

Fig. 5.3.
Histograms for Normalized Strength and the Theoretical Density Function for groups A to G.

From Fig. 4.12 very high β values would follow.

Even negative values of β which cannot be explained from the view point of physical processes involved are found. Only group H gives results which can be compated with eq. (5.3). The following reasons are considered to have a major influence on this unexpected descrepancy:

1. Paper pads between specimen and platens which served as thermal isolation might have influenced the actual rate of loading.
2. The temperature gradient between the center and the end of the specimens causes internal thermal stresses.
3. The rather soft loading frame, might prevent stress redistribution under high rate of loading.

Quantitative evaluation of the influence of environmental temperature on β needs to be done in the future. The preliminary tests described in this report are mainly meant to point out this problem.

6 Conclusions

The stochastic theory for fracture of concrete satisfactorily describes the experimental findings of strength as affected by rate of loading.

Bending and compressive strength of mortar and compressive strength of concrete increase with increase rate of loading.

Compressive strength seems to be influenced less severely by rate of loading than bending strength. Strength of weaker specimens is more affected by rate of loading.

The influence of rate of loading is satisfactorily described by a following power function:

$$\bar{\sigma}/\bar{\sigma}_0 = (\dot{\sigma}/\dot{\sigma}_0)^{\frac{1}{\beta+1}}$$

where $\bar{\sigma}_0$ and $\dot{\sigma}_0$ are reference mean value of strength and reference rate of loading respectively and β is a materials parameter.

β is found to be in the range between 17,8 and 22,3 for bending strength of mortar and between 25,3 and 27,5 for compressive strength of mortar and concrete. Light weight concrete shows a different behaviour in the range of high rates of loading. The reason for this phenomena should be investigated in the future.

The coefficient of variation is not influenced by rate of loading. On the basis of this, a distribution function of all strength values, normalized by the mean value for each rate of loading, can be obtained. The distribution function of strength is described satisfactorily by Weibull's distribution function. This applies both for strength as determined under bending load and under compressive load.

The distribution of strength of light weight concrete may be approximated by a Gaussian distribution function.

7 References

CAQUOT, M. and R. L'HERMITE, Les chocs et les charges dynamiques dans les constructions, Annales de l'Institut Technique du Bâtiment et des Travaux Publics, (1937).

CHANDON, H. C., R. C. BRADT and GR. E. RINDONE, Dynamic Fatigue of Float Glass, J. of the Am. Cer. Soc., **61,** 207 (1978).

EVANS, R. H., Effect of rate of loading on the mechanical properties of some materials, J. Inst. Civil Engin., **18,** 296 (1942).

FREUDENTHAL, A. M., Statistical approach to brittle fracture, Fracture, **II,** Academic Press, Ed. by H. Liebowitz (1968), p. 592.

GRIFFITH, A. A., The phenomena of rupture and flow in solids, Phil. Trans. Roy. Soc., **221,** Ser. A, (1920).

GUPTA, Y. M. and L. SEAMAN, Dynamic behaviour of reinforced concrete under missile impact loading, Proceedings ASCE Conference on Structural Design of Nuclear Plant Facilities, (1975).

HATANO, T., Dynamic behaviour of concrete under impulsive tensile load, Proc. Japan Soc. Civil Eng., **73,** (1961), (in Japanese).

HATANO, T., Theory of failure of concrete and similar brittle solid on the basis of strain, Proc. Japan Soc. Civil Eng. **153,** (1968), (in Japanese).

HIGGINS, D. D. and J. E. BAILEY, A microstructural investigation of the failure behaviour of cement paste, Proc. of a Conf. on "Hydraulic cement paste: their structure and properties", (1976) p. 283.

HUGHES, B. P. and R. GREGORY, Concrete subject to high rates of loading in compression, Mag. Concr. Research, **24,** 25 (1972).

KAPLAN, M. F., Crack propagation and the fracture of concrete, Journ. of Amer. Conc. Inst., **58,** (1961) p. 591.

LEEUWEN, J. VAN and A. J. SIEMES, Miner's rule with respect to plain concrete, Heron, **24,** 1, (1979).

MAINSTONE, R. J., Properties of materials at high rates of loading, Mater. et Constr., **44,** 102 (1975).

MAYNARD, D. P. and S. G. DAVIS, The strength of "in situ" concrete, The Structural Engineer, **52,** 10, (1974) p. 369–374.

MIHASHI, H. and M. IZUMI, A stochastic theory for concrete fracture, Cement and Concrete Research, **7,** 411 (1977).

REINHARDT, H. W., Uniaxial impact tensile strength of concrete, R.I.L.E.M. Symp. Brazil offshore '79, Rio de Janeiro, Vol. 7, 8 (1979).

SPARKS, P. R. and J. B. MENZIES, The effect of rate of loading upon the static and fatigue strengths of plain concrete in compression, Mag. Concr. Research, **25,** 83 (1973).

TAKEDA, J., H. TACHIKAWA and K. FUJIMOTO, Influence of straining rate and propagating stress wave on deformation and fracture of concrete, Proc. Second Int. Conf. on Mechanical Behaviour of Materials, Boston, (1976), p. 1468.

TORRENT, R. J., The log-normal distribution: A better fitness for the results of mechanical testing of materials, Matériaux et Constructions, **11,** 64, (1879), p. 235.

WATSTEIN, D., Effect of straining rate on the compressive strength and elastic properties of concrete, Amer. Concr. Inst., **49,** 729, (1953).

WEIBULL, W., A statistical theory of the strength of materials, Proc. Roy. Swedish Inst. of Eng. Res., **151,** (1939).

WITTMANN, F. H. and J. ZAITSEV, Verformung und Festigkeit poröser Baustoffe, Schriftenreihe Deutscher Ausschuss für Stahlbeton, Heft 232 (1973).

YOKOBORI, T., An interdisciplinary approach to fracture and strength of solids, Iwanami Book Co., (1974) (in Japanese).

ZECH, B. and F. H. WITTMANN, F. H., Influence of rate of loading on strength of concrete, (to be published), (1980).

ZECH, B. and F. H. WITTMANN, Dynamisches Verhalten einer Platte unter stossartiger Belastung, Cem. Concr. Res., **9,** 115–126 (1979).

Acknowledgement

This work was performed when H. Mihashi was a research fellow at the Delft University of Technology. We would like to thank Mr. Luijerink, Mr. Franken and Mr. Van der Ende for their assistance to the accomplishment of the experimental program.

Die diesem Bericht zugrunde liegenden Arbeiten wurden mit Mitteln des Bundesministeriums für Forschung und Technologie (Förderungskennzeichen 150201C) gefördert. Die Verantwortung für den Inhalt liegt jedoch allein bei den Autoren.

To our regret some errors have been crept into Volume 25 - 1980 - No. 3, Stochastic approach to study the influence of rate of loading on strength of concrete by H. Mihashi and F. H. Wittmann.

Correction

Page	Line	Error	Correction
3	9	buth	but
10	17	$\sqrt{\pi l \sigma}$	$\sqrt{\pi c^2 \sigma}$
11	eq. (2.8)	l: (l)	$\bar{l}$: $(\bar{l})$
11	eq. (2.9)	l	$\bar{l}$
13	eq. (2.23)	$\bar{p}_{li}$	$\bar{p}_{\delta i}$
	$\int$	$l = i - 1$	$\delta = i - 1$
	eq. (2.24)	L_l	L_δ
30	Fig. 3.5	ln N	log N
31	Fig. 3.6	1.8	1.0
35	1	or	of
47	2 from the bottom	low	high
51	Group B	0.2	0.6

G. J. van Alphen, secretary
Stevinweg 1
P.O. Box 5048
2600 GA Delft, The Netherlands